Energy, Mines and Resources Canada | Énergie, Mines et Ressources Canada

CANMET

Canada Centre for Mineral and Energy Technology | Centre canadien de la technologie des minéraux et de l'énergie

DIRECT MEASUREMENT OF ULTRASONIC ABSORPTION

J.P. MONCHALIN
NONDESTRUCTIVE TESTING SECTION

1984

This document is an unedited interim report prepared ... discussion and interpretation purposes. It does not represent a final expression of the opinion of the Canada Centre for Mineral and Energy Technology (CANMET)

Ce document est un rapport ... préparé et rédigé ... fin de discussion ... de documentation ... représente aucune ... opinion définitive de ... du Centre canadien de ... technologie des minéraux et de l'énergie (CANMET)

MINERALS RESEARCH PROGRAM

PHYSICAL METALLURGY RESEARCH LABORATORIES
REPORT: MRP/PMRL 84-88(TR)

MICROMEDIA

Projet no. 8351-231
82-231-001
Project CANMET/PMRL 360 081

"DIRECT MEASUREMENT OF ULTRASONIC ABSORPTION BY THERMO-ACOUSTIC AND THERMO-EMISSIVE TECHNIQUES"*

by

Jean-Pierre Monchalin
Physical Metallurgy Research Laboratories
CANMET, Energy, Mines & Resources Canada
Ottawa

July 20, 1982

* Work performed in the laboratories of the Industrial Materials Research Institute, National Research Council Canada.

Also performed in part at Ecole Polytechnique, Montréal with the collaboration of Prof. Lionel Bertrand.

The contribution of Dr. Jean Bussière by helpful discussions and suggestions, namely the Metglas ribbon experiment, is acknowledged.

I. INTRODUCTION

Nowadays, Non-Destructive Evaluation is not limited to the search of defects and cracks in materials, but also includes several techniques aiming at the non-destructive determination of several material properties. The properties of interest are primarily the mechanical properties of the material, so the techniques generally used are based on ultrasonics. So far, the development in this area has met very little practical success and, as of today, these new techniques are practically not used in the industry to determine mechanical properties. The main reason is their limited accuracy or reliability in the case of complexe materials, such as most steels used in practice.

In the case of metals, the properties one would like to determine are the yield strength, the tensile strength, the transition temperature, the hardness, the residual stresses, the state of fatigue... Some information on some of these parameters can be obtained by measuring ultrasonic attenuation and ultrasonic velocity. In particular, one should note that some success was obtained for ferritic-pearlitic steels by measuring ultrasonic attenuation : in this case, it was possible to predict with a relatively good accuracy yield and tensile strengths and the transition temperature [1]. At the basis of such determination, there is first the dependence of the attenuation on the grain size: attenuation includes an absorption term plus a scattering term, which varies theoretically as $d^3 f_u^4$ in the Rayleigh region (ultrasonic wavelength >> d), where d is the mean grain size and f_u the ultrasonic frequency. Secondly, this determination is based on the Hall-Petch relations which say that a mechanical property P varies as $P_o + C\ d^{-1/2}$ where P_o is dependent on the composition and C is a constant. One should also note that several correlations between measured mechanical properties (e.g. K_{1c}) and ultrasonic parameters have been reported in the litterature [2]. However this work is essentially empirical and a better understanding is required before expecting its generalization.

We propose instead to measure ultrasonic absorption. Since ultrasonic absorption depend upon several dislocation parameters (density and loop length) and since the mechanical properties of metals depend upon dislocation parameters and their change under applied stress, ultrasonic absorption is then related to several mechanical properties of a metal. Since ultrasonic absorption depend of two dislocation parameters, the density and the loop length, and since their are other causes of absorption [3, 4] (thermoelastic damping, heat flow between grains, magneto-elastic losses), we should not expect to get an absolute value of any material parameter solely from an absorption measurement. However, it seems reasonable to expect that one would be able to estimate the variation of a mechanical property, between several samples of the material manufactured in identical conditions or when a stress is applied. In particular, we should be able, at least in some cases, to measure the effect of cold work, residual stresses and to detect the onset of fatigue (before cracking). Concerning the measurement residual stresses by ultrasonic polarimetry, which has not yet been put into a practical use because of the complications produced by metal texture, we note that it has been proposed to use ultrasonic absorption to distinguish between anisotropy induced by stress and by texture [5].

Very little attention has been previously devoted to the use of ultrasonic absorption for NDE, mainly because absorption is not generally directly measured or easily deduced from conventional ultrasonic pulse-echo attenuation experiments. In some cases, it appears that ultrasonic absorption and ultrasonic scattering are well defined functions of grain size and ultrasonic frequency. In these cases, the absorption term can be deduced from attenuation measurements made at two ultrasonic frequencies [6]. Other data suggest that this is not always readily possible, the variation with grain size and frequency being not well defined [7, 8]. Furthermore, an attenuation measurement generally require a sample with precisely parallel surfaces, which is a serious limitation for practical and industrial applications.

We propose instead to measure directly ultrasonic absorption by measuring the amount of heat produced. To do that, it is necessary to use a very sensitive sort of thermometer, because ultrasonic absorption in metals is small and the ultrasonic power which can be used in practice is not very large. Contact temperature sensors (thermocouples, thermistors) should be excluded since heat would be generated by ultrasonic absorption by the binding agent and the sensor itself. Two systems which probe the surface temperature and measure the absorption to a depth of a few mm below the surface have been found attractive for this project and have been studied (see below). So far, we have not been able to devise a sufficiently sensitive thermometric system, which would probe deep inside a metal sample. This limitation to a measurement of near surface absorption may be considered as a drawback in some cases, but in the case of early detection of fatigue, it would be rather be an advantage, since surface and near surface phenomena generally dominate the evolution of fatigue [9].

In the work reported here, continuous ultrasonic excitation is applied to the sample. The beam intensity is modulated at a low frequency which can go from 0.01 Hz to 1 kHz. When a thermometer which monitors the surface temperature is used, the frequency of modulation determine the probing range, i.e. the range over which the absorption is measured. This range can be typically varied from a fraction of a mm to a few mm. It would also be possible to resort to internal modulation of the dislocations parameters by applying a low frequency oscillating stress($\ll$first yield stress) [10].

The proposed technique has several similarities with a technique known as vibrothermography [11]. In this technique, the sample studied is set into vibration or an ultrasonic wave is sent into it and the heat produced by the stresses around a defect is detected with an infrared camera. In the work presented here, we are rather concerned with the measurement of material properties rather than defect detection, although both orientations may become nearly identical, especially in the case of a fatigue experiment where cracks appear anyhow at some time during the cycling process.

Another difference is that we intend to detect changes of temperature several order of magnitude below the capability of an infrared camera.

This report is organized as follows. First, in section II, we recall several properties of heat diffusion in a periodic regime and introduce the notion of thermal waves. In section III, we derive an expression for the heat source produced by ultrasonic absorption. In section IV, we describe two thermometric systems and give the theory of their operation. In section V, we present several experimental results obtained with these types of thermometers and we present also an experiment demonstrating one use of the technique, namely the measurement of ultrasonic absorption in a Metglas ribbon located in a variable magnetic field. Finally in section VI, we conclude the first phase of this work and present briefly possible future developments.

II. HEAT DIFFUSION IN A PERIODIC REGIME AND THERMAL WAVES

(THEORETICAL ASPECT):

II. 1. Basic equations

Heat diffusion in a solid is expressed by the well known equation [12]:

$$K_s \nabla^2 T(\vec{r},t) + H(\vec{r},t) = \rho_s C_s \frac{\partial T(\vec{r},t)}{\partial t} \qquad (1)$$

where K_s, ρ_s, C_s are respectively the thermal conductivity, density, specific heat of the solid, $T(\vec{r}, t)$ is the temperature at point $\vec{r}$ and time t and $H(\vec{r}, t)$ the heat power density (W/m^3) of the source. This equation should be used with the appropriate boundary conditions for temperature and heat flux. In the case of a good thermal contact between the 2 media [1] and [2], the temperature and heat fluxes (normal components) are continuous (point $\vec{r}$ on the interface, normal oriented from 1 → 2) [12]:

$$T_1(t, \vec{r}) = T_2(\vec{r}, t) \qquad (2)$$

$$-K_1 \frac{\partial}{\partial n} T_1(\vec{r}, t) = -K_2 \frac{\partial}{\partial n} T_2(\vec{r}, t) \qquad (3)$$

If a source $S(\vec{r}, t)$ is localised on the interface, Eq 3 should be written:

$$S(\vec{r}, t) - K_1 \frac{\partial}{\partial n} T_1(\vec{r}, t) = - K_2 \frac{\partial}{\partial n} T_2(\vec{r}, t) \qquad (4)$$

In the case of an imperfect thermal contact, it is usual to characterize the contact by a parameter R, the thermal contact resistance defined by [12]:

$$\phi_{1\to2} = (T_1 - T_2)/R \qquad (5)$$

where T_1, T_2 are the temperatures across the interface and $\phi_{1\to2}$ is the heat flux from 1 → 2.

In a periodic regime at frequency $f(\omega = 2\pi f)$, using complex notations, $T(\vec{r}, t) = \text{Real}(\tau(\vec{r})e^{j\omega t})$, $H(\vec{r}, t) = \text{Real}(h(\vec{r})\ e^{j\omega t})$, Eq 1 can be written:

$$K_s \nabla^2 \tau + h = j\omega \rho_s c_s \tau$$

or

$$\nabla^2 \tau + \frac{h}{K_s} = \sigma_s^2 \tau \qquad (6)$$

where $\sigma_s = (1 + j)/\mu_s$, $\mu_s = \sqrt{2 K_s/\rho_s c_s \omega}$

μ_s, which is called the thermal diffusion length, represents the characteristic length of diffusion of heat during a period of the modulation. Values of μ_s for several materials are given in Table 1. In the unidimensional case, which is the only case we will consider in this report (this approximation is valid for an uniform source excitation or in the case where the detection system measures the average temperature across the surface), Eq 6 reduces to:

$$\frac{d^2\tau}{dz^2} + \frac{h(z)}{K_s} = \sigma_s^2 \tau \qquad (7)$$

This equation shows that the general solution for the complexe amplitude of the temperature modulation includes, besides the particular solution, two terms proportional to $e^{\sigma_s z}$ and $e^{-\sigma_s z}$. These two terms represent two <u>thermal waves</u>, the former propagating towards z negative and the latter towards z positive.

The solution of any problem can be found by solving Eq 6 (or Eq 7) with the appropriate boundary conditions Eq 2, Eq 3 (or Eq 4), Eq 5. In many cases of interest, the source term can be written

$$h(z) = h_o\ e^{-\alpha_p z} \qquad (8)$$

where α_p represents the absorption coefficient (power) of the incident beam (optical beam, electron beam or, for the case discussed here, ultrasonic beam). Therefore, in any medium (i) the solution for the temperature τ is:

$$\tau_i = A_o^{(i)} e^{-\alpha_p z} + A^{(i)} e^{\sigma_s z} + B^{(i)} e^{-\sigma_s z} \qquad (9)$$

Using the boundary conditions, $A_o^{(i)}$, $A^{(i)}$ and $B^{(i)}$ are solutions of a set of coupled equations and they can be determined either analytically for simple problems or numerically at a given frequency for more complex situations.

II. 2. Thermal waves

Alternatively, it is possible to consider thermal waves emitted by the source and to consider their reflexion, transmission and interference in a way similar to acoustics or optics. However, the distinctive feature of these waves is their highly damped nature, their damping length being equal to their propagation length (= μ_s). This wave approach gives results identical to the direct resolution of the diffusion equation with boundaries conditions. In order to apply this method, we have first to indicate how waves are produced by a pulsating heat source and then to calculate their transmission and reflexion at an interface (we limit ourselves to an unidimensional calculation, the time dependence $e^{j\omega t}$ is assumed implicitly everywhere):

a) Production of thermal waves by a pulsating source in an infinite medium

Let a thermal source of strength $\phi_o(W/m^2)$ be located at the origin.

From this source propagate a thermal wave $\tau_o e^{\sigma_s z}$ towards the negative z and $\tau_o e^{-\sigma_s z}$ towards the positive z. The application of Eq 4 yields:

$$\phi_o - K_s \sigma_s \tau_o = K_s \sigma_s \tau_o$$

then,
$$\tau_o = \frac{\phi_o}{2 K_s \sigma_s} \qquad (10)$$

These 2 waves (real part) are represented in Fig. 1.

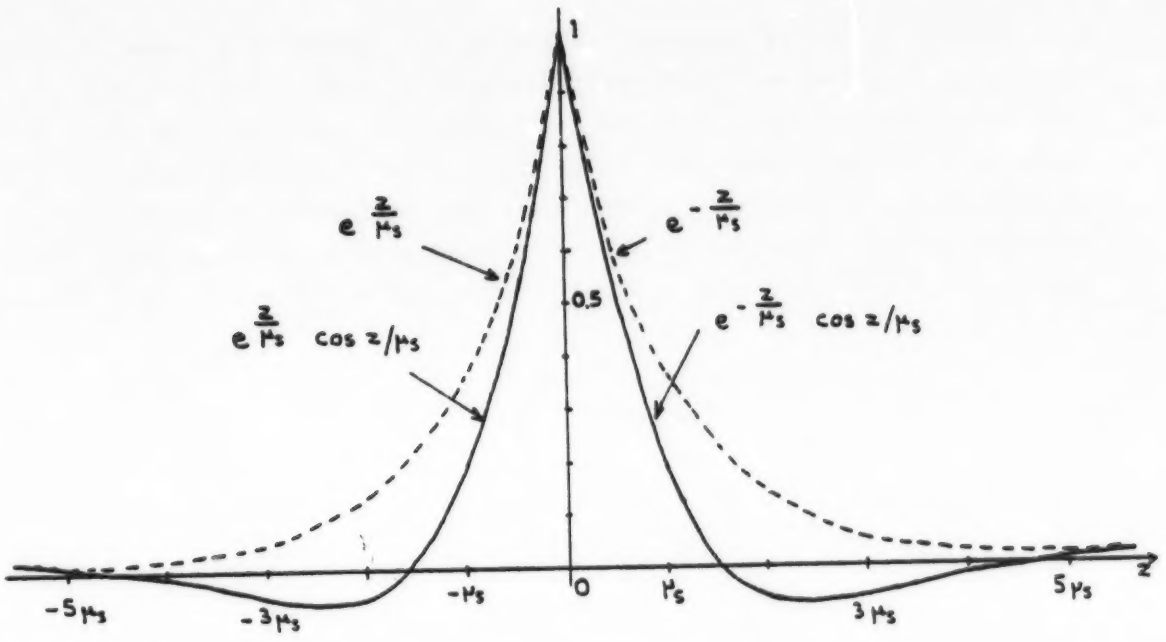

Fig. 1 Plot of the thermal waves produced by a source at z = 0 (exactly Real τ/τ_o)

Let us define as <u>thermal impedance</u> of the medium $R_s = 1/K_s\sigma_s$ (see Table 1). The reason of this denomination becomes obvious if we refer to Eq 5: like the parameter R which is introduced to describe an imperfect thermal contact, R_s is the ratio of a temperature ($\tau = \tau_o e^{-\sigma_s z}$) to a heat flux ($\phi = -K_s\, d\tau/dz = \tau_o K_s \sigma_s e^{-\sigma_s z}$). Eq 10 can be written:

$$\tau_o = \frac{R_s}{2}\,\phi_o \qquad (11)$$

In the case of a source located between two infinite mediums 1 and 2, we have:

$$\tau_o = \frac{1}{2}\,\phi_o \qquad (12)$$

In the case of an extended source, the thermal response can be obtained by summing the waves produced by elemental sources.

There is a strong mathematical similitude between these waves and strongly damped electromagnetic waves in a metal, used in the well known eddy currents technique. To show this similitude, let us consider a current sheet parallel in the y direction to the planar surface of a metal sample. In this case the induced magnetic field in the metal (there is only one component H_x) verifies the equation (13):

$$\frac{d^2 H_x}{d z^2} = \mu \sigma \frac{d H_x}{d t}$$

or at frequency $f(\omega = 2\pi f)$:

$$\frac{d^2 H_x}{d z^2} = j \omega \mu \sigma H_x \qquad (13)$$

μ is the permeability and σ the electric conductivity (the displacement current term has been neglected, since for metals $\sigma >> \omega\epsilon$, where ϵ is the electric permittivity). Eq 13 is similar to equation 6 or 7 (source h = 0): $H_x \leftrightarrow \tau$. The solution of Eq 13 is the well known damped electromagnetic wave [13]:

$$H_x = H_x(z = 0) \; e^{-\frac{1+j}{\delta} z} \qquad (14)$$

where δ is the penetration depth (analogous to μ) and is given by:

$$\delta = \sqrt{\frac{2}{\mu \sigma \omega}} \qquad (15)$$

b) <u>Transmission and reflexion of thermal waves</u>

Let us consider an interface between 2 media (1) and (2). τ_i, τ_R and τ_T are respectively the incident, reflected and transmitted waves (see Fig. 2). The application of the boundary conditions (Eq 2 and 3) yields:

$$\tau_i + \tau_R = \tau_T \qquad (16)$$

$$-K_1 \frac{d}{dz}(\tau_i + \tau_R) = -K_2 \frac{d}{dz}(\tau_T)$$

Since τ_i varies as $e^{-\sigma_1 z}$, τ_R as $e^{\sigma_1 z}$ and τ_T as $e^{-\sigma_2 z}$, this last equation can be written:

$$K_1\sigma_1\tau_i - K_1\sigma_1\tau_R = K_2\sigma_2\tau_T$$

or

$$\frac{\tau_i - \tau_R}{R_1} = \frac{\tau_T}{R_2} \qquad (17)$$

It then follows that the reflexion coefficient $r = \tau_R/\tau_i$ and the transmission coefficient $t = \tau_T/\tau_i$ are given by:

$$r = \frac{R_2 - R_1}{R_2 + R_1} \qquad (18)$$

$$t = \frac{2R_2}{R_2 + R_1} \qquad (19)$$

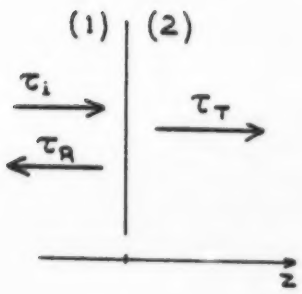

Fig. 2

In the case of an interface characterized by a thermal resistance R, it can be easily shown using Eq 5 and 17 that:

$$r = \frac{R + R_2 - R_1}{R + R_2 + R_1} \qquad (20)$$

$$t = \frac{2 R_2}{R + R_2 + R_1} \qquad (21)$$

II. 3. Calculation of the surface temperature modulation produced by a weakly absorbed beam

We presents in this section a direct application of the thermal wave formalism to the calculation of the surface temperature. The result of this calculation will be used further on in this report. The absorption coefficient of an ultrasonic beam ($\sim$ 10 MHz) varies between a few hundred m^{-1} (plastics) to a fraction of m^{-1} (fused quartz). For steel it is typically between 3 m^{-1} to 40 m^{-1} (see Table 1). Therefore, $\alpha << \sigma$, we can assume in good approximation that the heat source is practically uniform; we note it h_o (W/m^3). The temperature modulation at the surface solid gas can be calculated by summing an infinity of thermal waves:

$$\tau(0) = t_{s \to gas}\ h_o\ \frac{R_s}{2} \int_{-\infty}^{0} e^{\sigma_s z'} dz'$$

$$\tau(0) = \frac{2 R_g}{R_s + R_g}\ h_o\ \frac{R_s}{2\sigma_s}$$

$$\tau(0) = \frac{h_o}{1+\vartheta}\ \frac{1}{j\omega \rho_s C_s} \qquad (22)$$

where $\vartheta = \frac{R_s}{R_g} = \frac{K_g \sigma_g}{K_s \sigma_s}$ is generally small (see Table 1). We have used the identity $K_s \sigma_s^2 = j\omega \rho_s C_s$.

III. EXPRESSION OF THE HEAT SOURCE PRODUCED BY ULTRASONIC ABSORPTION

In the set up considered in this work, ultrasonic waves are launched normally to the surface and there is a creation of a standing wave in the sample: see Fig. 3.

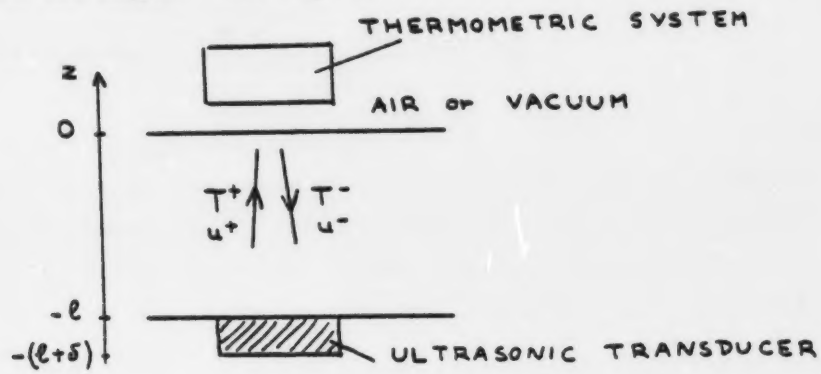

Fig. 3

The stress indident normally on the boundary (longitudinal or shear) can be written:

$$T^+ = A\, e^{-\alpha_{at} z} \sin(\omega_u t - k_u z) \qquad (23)$$

where $\omega_u = 2\pi f_u$, f_u is the ultrasonic frequency, k_u is the ultrasonic wave number ($= \omega_u/v$, where v is the longitudinal or shear velocity), α_{at} is the attenuation coefficient for the stress or strain (for the ultrasonic intensity, attenuation coefficient $= 2\ \alpha_{at}$), $\alpha_{at} = \alpha + \alpha_{sc}$, where α is the absorption coefficient and α_{sc} is the scattering coefficient, A is the stress amplitude of the incoming wave at $z = 0$. In order to calculate the ultrasonic intensity distribution inside the sample we can neglect the sound transmitted to the adjacent gas. Then the reflected stress wave can be written:

$$T^- = -A\, e^{\alpha_{at} z} \sin(\omega_u \tau + k_u z) \qquad (24)$$

Eq 23 and 24 verify at $z = 0$, $T^+ + T^- = 0$. The corresponding displacements can be written [14]:

$$u^+ = \frac{A}{\omega_u \nu \rho} e^{-\alpha_{at} z} \cos(\omega_u t - k_u z) \quad (25)$$

$$u^- = \frac{A}{\omega_u \nu \rho} e^{-\alpha_{at} z} \cos(\omega_u t + k_u z) \quad (26)$$

where ρ is the sample material density and we have used the fact that $\alpha << k_u$. Let us defined U as displacement amplitude at z = 0 (further on in this report, we will make U a slow varying function of t → U(t)). This amplitude can be measured by optical interferometry [15, 16] (U is twice the displacement produced by the incident ultrasonic stress alone):

$$U = \frac{2A}{\omega_u \nu \rho} \quad (27)$$

The ultrasonic energy flux I (or intensity) [14] is the sum of the intensities of the 2 beams I^+ and I^-:

$$I = I^+ + I^- = -T^+ \frac{\partial u^+}{\partial t} - T^- \frac{\partial u^-}{\partial t} = -(T^+ + T^-) \frac{\partial (u^+ + u^-)}{\partial t}$$

Taking the time average, we find:

$$< I > = \frac{\omega_u^2 Z}{8} U^2 \left(e^{-2\alpha_{at} z} - e^{2\alpha_{at} z}\right) \quad (28)$$

where Z = ρv is the material impedance (longitudinal or shear). < I > represents only the coherent part of the ultrasonic intensity. Scattering causes also some ultrasonic energy to be present as diffuse (incoherent). We assume at the initial stage of this project that the heat source originates mostly from the coherent part < I > and that the contribution from the scattered intensity is negligible. This is valid as we show below if an ultrasonic frequency in the low MHz range is used. For

example, for ferritic and austenitic steels α_{sc} is quoted to be $\sim 13\ d^3\ f_u^4\ (m^{-1})$ for shear waves [6], where d is mean grain size (in mm) and f_u is the ultrasonic frequency (in MHz). If the sample thickness ℓ is 1 inch, the contribution of scattering can be considered negligible when α_{sc} is much less than 20 m^{-1} ($2\ \alpha_{sc}\ \ell \ll 1$): this occurs for grain size as large as 200 μm (ASTM 2) at $f_u < 2.5$ MHz and at a higher frequency for smaller grain size. In the case of a compressional wave, a higher frequency can even be used, since the scattering coefficient is lower: for steels, α_{sc} (SHEAR) $\sim 4.6\ \alpha_{sc}$ (LONG).

The ultrasonic energy dissipated per unit length by absorption or scattering from the coherent beam equal to $-d\langle I\rangle/dz$. Since we neglect the heat produced by the diffuse beam, the heat source density h(z) is then obtained by taking the absorption contribution in the expression of $-d\langle I\rangle/dz$. It then follows:

$$h(z) = \frac{\alpha\, Z\, \omega_u^2\, U^2}{4} \left(e^{-2\alpha_{at} z} + e^{2\alpha_{at} z}\right) \qquad (29)$$

For the cases of interest here, $\alpha \ll 1/\ell$, where ℓ is the sample thickness or $\alpha \ll \sigma_s$, then $e^{-2\alpha z} + e^{2\alpha z} \sim 2$ and:

$$h = \alpha\, \frac{Z\, \omega_u^2\, U^2}{2} \qquad (30)$$

In this work, the ultrasonic stress or strain are modulated at a low frequency f ($\omega = 2\ \pi\ f$). We then write the amplitude as $U(t) = U\ (1 + \cos\ \omega t)/2$, where now U represents the maximum surface displacement at $z = 0$. Since $(1 + \cos\ \omega t)^2 = 3/2 + 2 \cos \omega t + \cos 2\ \omega t\ /\ 2$; the detected temperature modulation presents terms at the fundamental and the second harmonic of the modulation frequency. The time varying part of the heat source density can then be written:

$$h = \frac{\alpha Z \omega_u^2 U^2}{4} \cos \omega t + \frac{\alpha Z \omega_u^2 U^2}{16} \cos 2\omega t \qquad (31)$$

Several typical values of the absorption coefficient α are given in Table 1. We give below an order of magnitude for U, knowing that $Z\ \omega_u^2\ U^2/8$ represents the intensity given by the ultrasonic transducer in the case of weak absorption and scattering. For steel $Z_L \sim 4.7 \times 10^7$ kg.m.$^{-2}$.s^{-1}, at f_u = 10 MHz an intensity of 10 W/cm^2 corresponds to U $\sim$ 20 Å, and at f_u = 1MHz the same displacement amplitude is produced by an intensity $\sim$ 0.1 W/cm^2. Such amplitudes can easily been measured by optical interferometry, especially since the detection bandwidth can be made very narrow around the ultrasonic frequency [15, 16]. Therefore, when the scattered power can be neglected, the ultrasonic power coupled into the probed region can be easily measured.

The heat source can be increased considerably by mechanical resonance of the sample. This can occur when the sample has parallel faces and when α_{at} is sufficiently weak. We present below a derivation which expresses the heat source density as a function of the voltage applied to the transducer and shows this resonance effect. The derivation uses a simplified model for a piezoelectric transducer [17] (compression or shear): the stress T_p is related to the strain $\partial u_p/\partial z$ and the electric field E or the strain $\partial u_p/\partial z$ and the electrical displacement D by:

$$T_p = c^E \frac{\partial u_p}{\partial z} - eE \qquad (32)$$

$$T_p = c^D \frac{\partial u_p}{\partial z} - \frac{e}{\varepsilon^S} D \qquad (33)$$

when c^E, c^D are rigidity constants, e is a piezoelectric constant and ε^S is a dielectric constant. Using complex notations ($e^{i\omega t}$ implicit) the displacement in the transducer is written:

$$u_p = a_p e^{-ik_p z} + b_p e^{ik_p z} \qquad (34)$$

where k_p is the propagation constant inside the transducer, a_p and b_p are constants. It can be shown [17], for a piezoelectric material with moderate electromechanical coupling coefficient $e/\sqrt{\epsilon^S c^D k_p \delta}$ (δ is the transducer thickness, this applies in good approximation to quartz, in fair approximation to lithium niobate but not to PZT-5), that the stress is given is good approximation by:

$$T_p = -i\omega_u Z_p (a_p e^{-ik_p z} - b_p e^{ik_p z}) - e \frac{V_o}{\delta} \qquad (35)$$

where Z_p is the piezoelectric material impedance ($Z_p = k_p c^D/\omega_u$) and $V_o e^{i\omega t}$ is the voltage applied to the transducer. In the sample medium, the displacement is given by Eq 25, 26 and 27:

$$u = \frac{U}{2} (e^{-\beta z} + e^{\beta z}) \qquad (36)$$

where $\beta = \alpha_{at} + ik_u$.

Eq 23, 24 and 27 give for the stress:

$$T = -i\omega_u Z \frac{U}{2} (e^{-\beta z} - e^{\beta z}) \qquad (37)$$

We write below that $T_p = 0$ at $z = -\ell - \delta$ and the continuity displacement and stress at $z = -\ell$ (see Fig. 3):

$$-i\omega_u Z_p (a_p e^{ik_p(\ell+\delta)} - b_p e^{-ik_p(\ell+\delta)}) = e \frac{V_o}{\delta} \qquad (38)$$

$$a_p e^{ik_p \ell} + b_p e^{-ik_p \ell} = \frac{U}{2} (e^{\beta \ell} + e^{-\beta \ell}) \qquad (39)$$

$$-i\omega_u Z_p\left(a_p e^{ik_p\ell} - b_p e^{-ik_p\ell}\right) - e\frac{V_0}{\delta} = -i\omega_u Z\frac{U}{2}\left(e^{\Lambda\ell} - e^{-\Lambda\ell}\right) \quad (40)$$

After elimination of a_p and b_p it follows:

$$\frac{U}{2}\left[\mathcal{Z}\, e^{(\alpha_{at}+ik_u)\ell} - \mathcal{Z}^* e^{-(\alpha_{at}+ik_u)\ell}\right] = \frac{-i\,e\,V_0}{\omega_u\,\delta}\,\frac{\left(1-e^{ik_p\delta}\right)^2}{1+e^{2ik_p\delta}} \quad (41)$$

where $\mathcal{Z} = Z + i\,Z_p \tan k_p\delta = |\mathcal{Z}|\, e^{i\phi}$. Then U^2 is calculated (the phase origin is chosen to be that of the surface displacement) and substituted into Eq 29. It then follows ($h = h(0)$):

$$h(z) = \frac{\alpha\, e^2 |V_0|^2}{4\,\delta^2}\,\frac{Z}{|\mathcal{Z}|^2}\,\frac{\sin^4 k_p\delta/2}{\cos^2 k_p\delta}\,\frac{\cosh 2\alpha_{at} z}{\cosh 2\alpha_{at}\ell - \cos(2k_u\ell+\phi)} \quad (42)$$

$$h = \frac{\alpha\, e^2 |V_0|^2}{4\,\delta^2}\,\frac{Z}{|\mathcal{Z}|^2}\,\frac{\sin^4 k_p\delta/2}{\cos^2 k_p\delta}\,\frac{1}{\cosh 2\alpha_{at}\ell - \cos(2k_u\ell+\phi)} \quad (43)$$

For weak attenuation $2\,\alpha_{at}\,\ell \ll 1$, $\cosh 2\,\alpha_{at}\,\ell \sim 1 + 2\,\alpha_{at}^2\,\ell^2$, h shows a large increase for $2\,k_u\,\ell + \phi = \pi + 2\,m\pi$ (m integer) or $\ell = \frac{\lambda_u}{4} + m\,\frac{\lambda_u}{2} - \frac{\phi}{4\pi}\,\lambda_u$. In order to get a strong signal, the sample should be excited at one of these resonance frequencies. In this case, the signal may depend critically on the value of the frequency so it would be necessary to monitor U by optical interferometry in order to measure α.

When the transducer is excited at half-wave resonance as it is often the case $k_p\,\delta = \pi$, $\phi = 0$, $\mathcal{Z} = Z$, Eq 42 and 43 simplify accordingly:

$$h(z) = \frac{\alpha e^2 |V_o|^2}{4\delta^2 Z} \quad \frac{\cosh 2\alpha_{at} z}{\cosh 2\alpha_{at} \ell - \cos 2k_u \ell} \tag{44}$$

$$h = \frac{\alpha e^2 |V_o|^2}{4\delta^2 Z} \quad \frac{1}{\cosh 2\alpha_{at} \ell - \cos 2k_u \ell} \tag{45}$$

When the sample does not have parallel surfaces, the piezoelectric transducer being a phase sensitive device, the interference effect of the 2 counter-propagating waves (see the terms on the left hand side of Eq 41) averages out after integration over the transducer surface. In this case the cosin term in denominator disappears and the expressions for the heat source reduce to:

$$h(z) = \frac{\alpha e^2 |V_o|^2}{4\delta^2} \quad \frac{Z}{|Z|^2} \quad \frac{\sin^4 k_p \delta/2}{\cos^2 k_p \delta} \quad \frac{\cosh 2\alpha_{at} z}{\cosh 2\alpha_{at} \ell} \tag{46}$$

$$h = \frac{\alpha e^2 |V_o|^2}{4\delta^2} \quad \frac{Z}{|Z|^2} \quad \frac{\sin^4 k_p \delta/2}{\cos^2 k_p \delta} \quad \frac{1}{\cosh 2\alpha_{at} \ell} \tag{47}$$

IV. DESCRIPTION AND THEORY OF SEVERAL THERMOMETRIC SYSTEMS

In order to measure the heat produced by the absorption of ultrasound, we need some kind of thermometer. This thermometer should measure the amplitude of the temperature modulation (we operate with an intensity modulated ultrasonic beam) at some location inside the sample or throughout the sample. Two devices which probe the surface temperature of the sample and, therefore, measures the ultrasonic absorption within a surface layer of thickness equal about to the thermal diffusion length ($\sim$ 2 mm in carbon steel) have been used and are first described. One of them uses a microphone and measures the pressure modulation of a gas filled cell mounted on the sample. The other one uses an infrared detector and measures the emissivity of the surface. The former will be described first since its theory of operation can be readily used to deduce that of the latter. We are also briefly considering several systems which probe the temperature modulation inside the sample. They have not been tried and they need further consideration. One of the main difficulty lies in the fact that the thermometer should not detect the heat source produced by the transducer or the coupling fluid. This source can be quite strong since ultrasound is absorbed very strongly by coupling fluids such as water, oil or grease. This effect can be minimized by operating at a lower ultrasonic frequency, since ultrasonic absorption in metals generally scales as f_u, whereas in liquid it scales as f_u^2. In practice, when probing the surface temperature, this problem is avoided by having the probed region several μ_s (5 to 10) away from the exciting transducer, so the thermal wave originating from the transducer is highly damped before reaching the probed aera.

IV. 1. Detection with a cell filled by a gas applied onto the sample and a microphone

A schematic of the setup is shown in Fig. 4 (μ_s is the thermal diffusion length of the solid, μ_g is that of the gas).

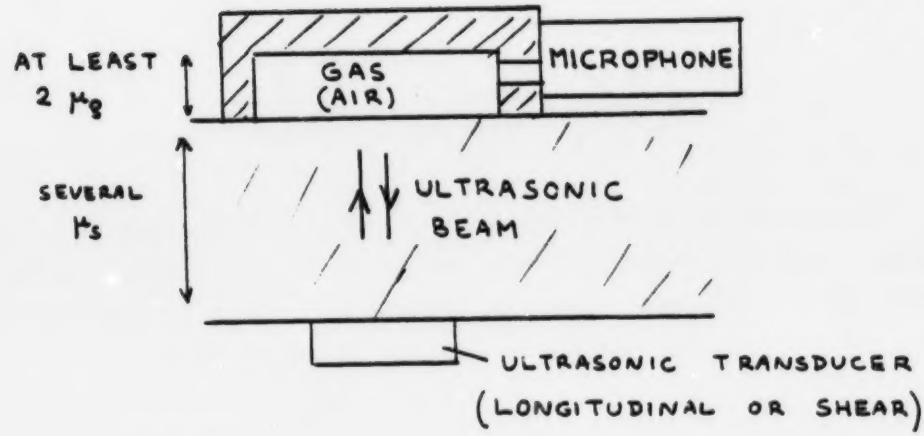

Fig. 4

This setup is quite similar to the one used in photoacoustics: in the case of the present work, the heat source is produced by the absorption of the ultrasonic beam instead of that of an optical beam illuminating the surface of the sample. In both cases, the pressure modulation is directly proportional to the surface temperature modulation. When the cell has a sufficiently large size, (depth at least $\sim 2\ \mu_g$), the phenomenon in the gas can be viewed as the periodic expansion of a surface gas layer which acts adiabatically as a piston upon the remaining gas [17]. The pressure modulation p at frequency f is then related to the surface temperature $\tau(0)$ by [18]:

$$P = \frac{\gamma P_o}{T_o V_g} \frac{S\,\tau(0)}{\sigma_g} \qquad (48)$$

where P_o, T_o are respectively the ambiant pressure and ambiant temperature, γ is the ratio of the specific heats of the gas at constant pressure and constant volume , V_g is the cell volume, S is the area of the sample heated by the ultrasonic beam (assumed

to be less than the cell cross-section). $\tau(0)$ is given by Eq 22 with $h_o = \alpha Z \omega_u^2 U^2/4$ (see Eq 31), where Z is the acoustic impedance of the solid sample. Then,

$$P = \frac{\gamma P_o S}{j\omega T_o V_g} \frac{\omega_u^2 U^2}{(1+g)\sigma_g} \frac{\alpha Z}{4 \rho_s C_s} \tag{49}$$

This equation corresponds only to the periodic expansion of the gas; there is also a periodic expansion of the sample. ℓ being the sample thickness, $\delta\ell$ the modulation of thickness and β_s the thermal expansion coefficient of the sample, we can write:

$$\frac{d\ell}{dt} = j\omega \delta\ell = \ell \beta_s \frac{d\tau}{dt} \tag{50}$$

$$\rho_s C_s \frac{d\tau}{dt} = \alpha Z \omega_u^2 U^2/4 \tag{51}$$

It then follows:

$$\delta\ell = \frac{\ell \beta_s}{j\omega} \frac{\alpha Z \omega_u^2 U^2}{4 \rho_s C_s} \tag{52}$$

If we assume that the sample is free on both sides (cell side and transducer side with the coupling fluid layer) and that cell walls are fixed, the change of volume of the gas is $-\delta\ell S/2$. This corresponds to a pressure signal

$$P = \gamma P_o \frac{\delta\ell S/2}{V_g} \tag{53}$$

Then, by combining Eq 49, 53 and 52, it results:

$$p = \frac{\gamma P_o S}{j\omega V_g} \frac{\alpha Z \omega_o^2 U^2}{4 \rho_s C_s} \left[\frac{\ell \beta_s}{2} + \frac{\mu_g}{(1+j)(1+g) T_o} \right] \quad (54)$$

The thermal expansion of the sample is generally small by comparison with the gas expansion term. For the plexiglas sample used in this project (see next section), $\ell \sim 5.72$ mm, $\beta_s \sim 6 \times 10^{-5}$ $°K^{-1}$, $\ell \beta_s / 2 \sim 1.7 \times 10^{-4}$ mm/°K (for carbon steel $\beta_s \sim 1.1 \times 10^{-6}$ $°K^{-1}$). If the cell is filled by air, $\mu_g T_o \sim 2.7 \times 10^{-3}$ mm/°K at 10 Hz (even larger in the case of helium). Then, $\ell \beta_s / 2 \ll \mu_g / T_o$ in general. Furthermore, since the probed aera does not expand freely and the cell walls are not completely fixed, the effect of the sample expansion is even smaller. If the ultrasonic beam fills nearly completely the cell cross-section, the effect is certainly quite negligible (see Fig. 5).

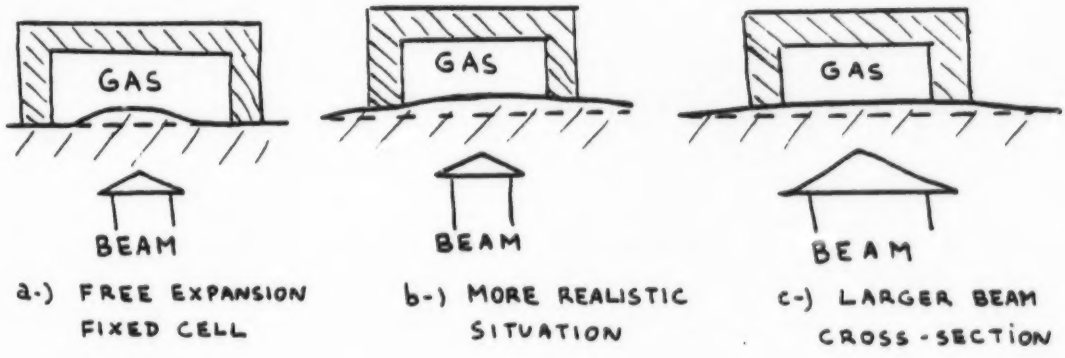

Fig. 5 Effect of the sample thermal expansion. The dash line represents the undisturbed sample surface.

Therefore, the appropriate expression reduces to Eq 49. But, we have neglected the ultrasonic transmission into the gas. The transmitted beam is very weak but it is strongly absorbed, as well in the case of a compressional wave (because of the high frequency involved, see Table 1) as in the case of a shear wave (there cannot be propagation of a shear wave into a fluid, the wave is localized

near a solid boundary and is heavily damped). Furthermore, the specific heat per unit volume of a gas being much less than that of a solid the weak heat source produced by ultrasonic absorption in the gas may result into a significant temperature modulation. Therefore, it is necessary to calculate this effect. We first give below an expression for the heat source in the case of a compressional wave at normal incidence, then we calculate the heat source for a shear wave at normal indicence.

In the case of compressional wave at normal incidence, the transmitted displacement can be written $U(t)\ e^{-\alpha_g z}\ .\ \cos(\omega_u t - k_{gu} z)$, where α_g is the ultrasonic absorption coefficient of the gas and k_{gu} its propagation constant at the ultrasonic frequency f_u ($= \omega_u/2\pi$). Then the time averaged intensity is [19] $Z_g\ U^2(t)\ \omega_u^2\ e^{-2\alpha_g z}/2$. If $U(t) = U\ (1 + \cos \omega t)/2$, the heat source density (W/m^3) h_g in the gas at the fundamental modulation frequency ω is given by (see section III):

$$h_g = \alpha_g \frac{Z_g}{2} \omega_u^2 U^2 e^{-2\alpha_g z} \qquad (55)$$

In the case of a shear wave at normal incidence, the transmitted displacement in the gas, assuming perfect accomodation at the surface (no gas slip), can be written [20] $U(t)\ e^{-z/\mu_v} \cos(\omega_u t - z/\mu_v)$, where μ_v is the viscous typical length and is equal to $\sqrt{2\,\eta/\rho_o \omega_u}$ (η is the shear viscosity coefficient of the gas and ρ_o is the gas density). μ_v is approximatively equal, obviously, to μ_g for the same frequency: $\mu_v \sim 2.054/\sqrt{f_u}$ mm^{-1} for air at atmosphere pressure and $\mu_v \sim 5.735\ /\ \sqrt{f_u}$ mm^{-1} for helium at atmospheric pressure. The corresponding shear stress is [20] $\eta \frac{\partial}{\partial z} \frac{\partial}{\partial t}$(displ.) $=$ Real $\left\{ \eta\ U(t)\ \omega_u \frac{1-j}{\mu_v}\ e^{\left(j\omega_u t - \frac{1+j}{\mu_v} z\right)} \right\}$. The intensity is equal to -stress $\times \frac{\partial}{\partial t}$(displ.) [14]. Taking the time average it results: $U^2(t)\ \omega_u^2 \frac{\eta}{2\mu_v} e^{-2z/\mu_v}$. Since $U(t) = U(1 + \cos\omega t)/2$, the heat source density at ω is given by:

$$h_g = (1/\mu_v)\,\frac{\eta}{2\mu_v}\,\omega_u^2\,U^2\,e^{-2z/\mu_v} \qquad (56)$$

This equation is identical to Eq 55, if we identify $1/\mu_v$ to α_g and η/μ_v to Z_g. $1/\mu_v$ and η/μ_v are given in Table 1 in the columns of α_{SHEAR} and Z_{SHEAR} for f_u = 5 MHz.

The basic equations of the problem are written below: Eq 7 (rewritten as Eq 57) applies to the solid sample, Eq 58 and 59 describe the thermal and acoustic behaviour of the gas [20, 21]:

$$\frac{d^2\tau_s}{dz^2} - \sigma_s^2\tau_s + \frac{h_s}{K_s} = 0 \qquad (57)$$

$$\frac{d^2\tau_g}{dz^2} - \sigma_g^2\tau_g + \frac{h_g}{K_g} = -j\omega\,\frac{p}{K_g} \qquad (58)$$

$$\frac{d^2p}{dz^2} + \gamma k_o^2 p = \frac{\gamma k_o^2 P_o}{T_o}\,\tau_g \qquad (59)$$

where k_o is the acoustic propagation constant at ω: $k_o = \omega\sqrt{\rho_o/\gamma P_o}$, ρ_o being the gas density; h_g is given by Eq 55 or 56 and $h_s = \alpha\, Z\, \omega_u^2\, U^2/4$ (see Eq 31). The solutions of these equations are:

$$\tau_s = b\,e^{\sigma_s z} + \alpha\, Z\,\omega_u^2\,U^2/(4\,K_s\,\sigma_s^2) \qquad (60)$$

$$\tau_g = a\,e^{-\sigma_g z} + \tau_{ac} + c\,e^{-2\alpha_g z} \qquad (61)$$

$$p = A\,e^{-jk_o z} + B\,e^{jk_o z} + p_{th} + d\,e^{-2\alpha_g z} \qquad (62)$$

where a, b, c, d, A and B are constants. τ_{ac} and p_{th} represent

the temperature term of the acoustical mode ($e^{-jk_o z}$ and $e^{jk_o z}$ terms) and the pressure term of the thermal mode ($e^{-\sigma_g z}$ term), respectively [21, 22]. We have assumed that the gas cell length ℓ_g is >> μ_g, so there is no $e^{\sigma_g z}$ term in Eq 61. c and d are determined by substitution into Eq 58 and 59:

$$\left(4\alpha_g^2 - \sigma_g^2\right) c + \frac{\alpha_g Z_g \omega_o^2 U^2}{2 K_g} = -\frac{j\omega}{K_g} d \tag{63}$$

$$\left(4\alpha_g^2 + \gamma k_o^2\right) d = \frac{\gamma k_o^2 P_o}{T_o} c \tag{64}$$

Since $k_o^2 << \alpha_g^2$, it follows:

$$c \sim \frac{\alpha_g Z_g \omega_o^2 U^2}{2 K_g \left(\sigma_g^2 - 4\alpha_g^2\right)} \tag{65}$$

$$d \sim \frac{\gamma k_o^2}{4\alpha_g^2} \frac{P_o}{T_o} c \tag{66}$$

For the same reason, it follows from Eq 58:

$$\tau_{ac} \sim \frac{1}{\rho_o c_p} \left(A e^{-jk_o z} + B e^{jk_o z}\right) \tag{67}$$

and from Eq 59:

$$P_{th} \sim \frac{\gamma P_o k_o^2}{T_o \sigma_g^2} a e^{-\sigma_g z} \tag{68}$$

The remaining constants a, b, A and B are determined by the

boundary conditions, Eq 69, 70 and 71, at the surface of the sample (z = 0) and the boundary condition, Eq 72, at the end of the cell ($z = \ell_g$). These conditions express the continuity of temperature and heat fluxes and that the gas velocity vanishes on the sample (neglecting its weak periodic expression) and on the cell walls:

$$b + \frac{\alpha Z \omega_u^2 U^2}{4 j\omega \rho_s C_s} = a + \frac{A+B}{\rho_o C_p} + \frac{\alpha_g Z_g \omega_u^2 U^2}{2 K_g (\sigma_g^2 - 4\alpha_g^2)} \qquad (69)$$

$$-b K_s \sigma_s = a K_g \sigma_g + K_g \frac{j k_o}{\rho_o C_p}(A-B) + \frac{\alpha_g^2 Z_g \omega_u^2 U^2}{\sigma_g^2 - 4\alpha_g^2} \qquad (70)$$

$$-j k_o (A-B) - \frac{\gamma P_o k_o^2}{T_o \sigma_g} a - 2\alpha_g \frac{\gamma k_o^2}{4\alpha_g^2} \frac{P_o}{T_o} \frac{\alpha_g Z_g \omega_u^2 U^2}{2 K_g (\sigma_g^2 - 4\alpha_g^2)} = 0 \qquad (71)$$

$$A e^{-j k_o \ell} - B e^{j k_o \ell} = 0 \qquad (72)$$

Since $k_o \ell \ll 1$ (cell size << acoustic wavelength at the audio frequency ω), it follows from Eq 72:

$$A - B \sim 2 j k_o \ell B \qquad (73)$$

$$A + B \sim 2 B \qquad (74)$$

Eq 73 and 74 are then substituted in Eq 69, 70 and 71. By eliminating b from Eq 69 and 70, it follows:

$$\frac{\alpha Z \omega_u^2 U^2}{4 j \omega \rho_s C_s} = a(1+g) + \frac{2B}{\rho_o C_p} - 2 \frac{K_g}{\rho_o C_p} \frac{k_o^2 \ell B}{K_s \sigma_s} + \frac{\alpha_g Z_g \omega_u^2 U^2}{\sigma_g^2 - 4\alpha_g^2}\left(\frac{1}{2K_g} + \frac{\alpha_g}{K_s \sigma_s}\right) \qquad (75)$$

In the right hand side of Eq 75, the third term is negligible with respect to the 2nd. We then eliminate a from Eq 75 and 71 in

order to get the detected pressure modulation which is practically uniform within the cell and equal to A + B ∿ 2 B. It follows:

$$2B\left(\ell + \frac{\gamma P_o}{T_o \sigma_g (1+g) \rho_o C_p}\right) = \frac{\gamma P_o}{T_o} \frac{\alpha Z \omega_o^2 U^2}{4 j \omega \rho_s C_s \sigma_g (1+g)} + \frac{\gamma P_o}{T_o} \frac{Z_g \omega_o^2 U^2}{4(1 - 4\alpha_g^2/\sigma_g^2)}$$

$$\times \left[\frac{1}{j\omega \rho_o C_p} - \frac{4\alpha_g}{(1+g)\sigma_g^3} \left(\frac{1}{2K_g} + \frac{\alpha_g}{K_s \sigma_s} \right) \right] \quad (76)$$

We define an effective volume $V_e = S \left(\ell + \frac{\gamma P_o}{T_o \sigma_g (1+g) \rho_o C_p}\right) = S\left(\ell + \frac{\gamma - 1}{(1+g)\sigma_g}\right)$

∿ V_g since $\ell >> \mu_g$.

Then, the detected signal is given by:

$$p = \frac{\gamma P_o S}{j\omega T_o V_e} \frac{\omega_o^2 U^2}{4\sigma_g} \left\{ \frac{\alpha Z}{(1+g)\rho_s C_s} + \frac{Z_g \sigma_g}{\rho_o C_p (1 - 4\alpha_g^2/\sigma_g^2)} \left[1 - \frac{2\alpha_g}{\sigma_g (1+g)} \left(1 + \frac{2\alpha_g K_g}{K_s \sigma_s} \right) \right] \right\} \quad (77)$$

We see that several terms which are caused by ultrasonic absorption by the gas have been added to Eq 49. These terms will be important when α is small. Eq 77 can be simplified if $2\alpha_g K_g / K_s \sigma_s$ is small. For a compression wave at 10 MHz, $2\alpha_g K_g / K_s \sigma_s$ amounts to (see Table 1) ∿ 4.7×10^{-2} x $(1-j)/\sqrt{f}$ for dry air and plexiglas, ∿ 2×10^{-3} x $(1-j)/\sqrt{f}$ for dry air and steel, ∿ 7.5×10^{-2} x $(1-j)/\sqrt{f}$ for helium and plexiglas, ∿ $3 \times 10^{-3}(1-j)/\sqrt{f}$ for helium and steel. Then, since also $g << 1$, Eq 77 reduces to:

$$p \sim \frac{\gamma P_o S}{j\omega T_o V_e} \frac{\omega_o^2 U^2}{4\sigma_g} \left\{ \frac{\alpha Z}{(1+g)\rho_s C_s} + \frac{Z_g \sigma_g}{\rho_o C_p} \frac{1}{1 + 2\alpha_g/\sigma_g} \right\} \quad (78)$$

For dry air (10 MHz) $2\alpha_g\mu_g \sim 9.7/\sqrt{f}$ and $Z_g/\rho_o C_p \mu_g \sim 132\sqrt{f}$; for helium (10 MHz) $2\alpha_g\mu_g \sim 7.3\sqrt{f}$ and $Z_g/\rho_o C_p \mu_g \sim 27\sqrt{f}$. For plexiglas (10 MHz), $\alpha Z/(1+g)\rho_s C_s \sim 188$ and for steel (10 MHz, $\alpha = 10\ m^{-1}$) $\alpha Z/(1+g)\rho_s C_s \sim 125$. These orders of magnitude show that the gas absorption term is not readily negligible. If a lower ultrasonic frequency is used, $2\alpha_g\mu_g$ is even smaller; it will then result, at least in the case of air, that the gas absorption term is as large as the sample absorption term, if not preponderant (depending on f). This calculation predicts also that the gas absorption effect is much smaller for helium than for air.

In the case of a shear wave at normal incidence, Eq 77 simplifies differently. In this case, $|2\alpha_g K_g/K_s\sigma_s| \geq 1$ and $|2\alpha_g/\sigma_s| \gg 1$ when $\alpha_g = 1/\mu_v$, then the 2nd term between brackets in Eq 63 reduces to $\frac{Z_g\, j\omega}{(1+g)2K_s\alpha_g}\left(1+\frac{2\alpha_g K_o}{K_s\sigma_s}\right)$. This term is less than $\sim Z_g\, j\omega/K_s\sigma_s = Z_g\sigma_s/\rho_s C_s$ where $Z_g = \eta/\mu_v$. Since $(\eta/\mu_v)\sigma_s$ is much less than αZ, the 2nd term is negligible by compression to the term linked to absorption by the sample.

Finally we give an estimate of the detection limit expected with the microphone thermometric system. We have measured the noise of the microphone 4144 (1 inch diameter) of Bruel & Kjaer with its preamplifier to be $\sim 3 \times 10^{-9}$ atm/Hz$^{1/2}$ at 2 Hz (its sensitivity is $\sim$ 50 mV/Pa or 5 KV/atm). According to Eq 48, if a cell of optimum volume is used (i.e. $\ell_g \sim \mu_g$), P/P_o is of the order of $\tau(0)/T_o$. In this case, it results a detection limit of $\sim 10^{-6}$ °C/Hz$^{1/2}$ at 2Hz. This figure means that, if we use a lock-in amplifier with a time constant of 10 sec. and a 12 db/oct. roll-off (bandwidth = 1/(8 x time ct.)), 10^{-7}°C can be detected.

IV. 2. Detection of the surface emissivity

This technique uses an infrared detector to measure the radiation flux emitted by the surface, which is a fonction of the surface temperature. Since the temperature modulation is small, the

detected signal is directly proportional to its amplitude $\tau(0)$. If the space between the detector and the sample surface has been evacuated, Eq 22 simply applies with $h_o = \alpha Z \omega_u^2 U^2/4$, then:

$$\tau(0) = \frac{\alpha Z \omega_u^2 U^2}{4 j \omega \rho_s C_s (1+g)} \tag{79}$$

Then, the surface temperature and the infrared signal vary with the modulation frequency as 1/f. Without evacuation of the space in front of the detector, there is transmission of an ultrasonic wave into the air. This wave is strongly absorbed and the produced heat may affect the surface temperature. The magnitude of this effect is calculated below using the derivation of section IV. 1. Eq 55 to 71 apply to this case, but since we are in free space B = 0. Eq 75 is now substituted by the following equation (neglecting one term as in Eq 75):

$$\frac{\alpha Z \omega_u^2 U^2}{4 j \omega \rho_s C_s} = a(1+g) + \frac{A}{\rho_o C_p} + \frac{\alpha_g Z_g \omega_u^2 U^2}{\sigma_g^2 - 4\alpha_g^2}\left(\frac{1}{2K_g} + \frac{\alpha_g}{K_s \sigma_s}\right) \tag{80}$$

In Eq 80, the term $A/\rho_o C_p = \tau_{ac}(0)$ can be neglected, as it can be seen if Eq 71 is used ($k_o \ll \sigma_g$, $k_o \ll \alpha_g$, we use the identity $\gamma P_o/T_o = (\gamma-1)\rho_o C_p$). Then, the surface temperature modulation is given by ($\tau(0) \sim a + c$, we neglect τ_{ac} for the same reason as above):

$$\tau(0) = \frac{\omega_u^2 U^2}{4 j \omega (1+g)} \left\{ \frac{\alpha Z}{\rho_s C_s} + \frac{2 \alpha_g Z_g g}{\rho_o C_p \left(1 + \frac{2\alpha_g}{\sigma_g}\right)} \right\} \tag{81}$$

This equation can be also readily obtained by neglecting the acoustical mode produced in the gas and solving only a thermal problem. When the experiment is performed in dry air at 10 MHz,

$2\alpha_g Z_g/\rho_o C_p \sim 1275$, $2\alpha_g \mu_g \sim 9.7 / \sqrt{f}$; for a plexiglas sample, $\gamma \sim 0.01$ and $\alpha Z/\rho_s C_s \sim 188$ (10 MHz); for a carbon steel sample, $\gamma \sim 4 \times 10^{-4}$ and $\alpha Z/\rho_s C_s \sim 125$ (10 MHz, $\alpha = 10\ m^{-1}$). These values show that absorption by air is generally negligible and that Eq 81 reduces to Eq 79, except for low α values ($\alpha < 1\ m^{-1}$) and a sufficiently high modulation frequency such that $2\ \alpha_g \mu_g < 1$. In the case of a shear wave at normal indicence, the second term between bracket reduces to $Z_g \sigma_g \gamma / \rho_o C_p$. $Z_g/\rho_o C_p \mu_g \sim 8.4 \sqrt{f}$ in air , $\gamma \sim 0.01$ for air and plexiglas and $\gamma \sim 4 \times 10^{-4}$ for air and steel. These values show that in this case the absorption by air is always negligible.

We now discuss the choice of the infrared detector and of the infrared wavelength detection bandwidth. This bandwidth $[\lambda_1, \lambda_2]$ should be such that $\int_{\lambda_1}^{\lambda_2} \partial L(\lambda)/\partial T \, d\lambda$, where $L(\lambda)$ is the radiance per unit spectral interval of the sample, is maximized. From black-body radiation theory, it follows that the optimum bandwidth for emission at room temperature is between 5 and 20 μm [23]: below 5 μm the emission is negligible and above 20 μm there is practically no increase of $\int_{\lambda 1}^{\lambda 2} \partial L(\lambda)/\partial T \, d\lambda$. Liquid nitrogen cooled detectors such as Mercury Cadmium Telluride (8-14 μm) or Lead Tin Telluride (6-13 μm) which have an excellent detectivity ($> 10^{10}$ cm $Hz^{1/2}/W$) can be used as detectors. However, the detecting element is generally small (∿ 1 mm squared) and has a rather large 1/f noise. It then follows that broad band thermal detectors, such as pyrolectrics TGS (Tri-glycine Sulfate) and the Golay detector which are currently manufactured up to 5 mm in diameter and operate well at low frequencies are better for the application considered here. The pyroelectric detector PI-75 (5 mm diameter) of Molectron Corp. has a NEP (Noise equivalent power) of 2×10^{-9} $W/Hz^{1/2}$ between 1 to 20 Hz [24], whereas the Golay detector has even a lower NEP (typically ∿ 10^{-10} $W/Hz^{1/2}$) for the same frequency interval and the same absorbing area [25]. The pyroelectric detector PI-75 has a much smaller physical size than the Golay and its absorbing surface is closer to its window, which, for measurements where the detector can be located very close to the

probed surface compensates in part for its lower detectivity. For the detector PI-75, the maximum viewing half-angle θ from the sample surface is about 50°, whereas for the Golay it is about 18°. Since the radiated flux is proportional to $1-\cos 2\theta$, this difference of solid angles represents a factor of about 6, so the Golay detector is better in this case only by a factor 3 to 4. In the case where the emitted radiation is collected through some optical system, the Golay detector is the best choice for the application considered.

We present below an estimate of the detection limit which can be expected with the detector PI-75 (with a black absorbing coating). The modulated radiation flux collected by the detector is given in good approximation by [22]:

$$\delta F = \varepsilon \frac{\partial}{\partial T}\left(K T^4\right) A_s \frac{\pi}{2}\left(1 - \cos 2\theta\right) \delta T \qquad (82)$$

where $K = 1.8 \times 10^{-8}$ W/m^2 sr^{-1} °K^{-4} (Stefan - Boltzman's constant)

A_s is the sample area viewed by the detector ($\sim \pi \times 5^2$ mm^2)

θ is the half viewing angle of the detector surface from the sample (5 mm in diameter at about [redacted] mm gives $\theta \sim$ 50°)

T is the absolute sample temperature and δT is its amplitude of modulation

ε is the sample emissivity.

In Eq 82, we have approximated $\frac{\partial}{\partial T}\int_{\lambda_1}^{\lambda_2} L(\lambda)d\lambda$ by $\frac{\partial}{\partial T}\int_0^\infty L(\lambda)\, d\lambda$ where $\int_0^\infty L(\lambda)\, d\lambda$ is the black-body radiance function (= K T^4). This approximation is excellent for a broad band detector such as the pyroelectric with a black coating. We find $\delta F \sim 2.6 \times 10^{-4}\ \varepsilon\ \delta T$ (W). This detector has a NEP of 2×10^{-9} W/Hz$^{1/2}$ which gives a detection limit of $10^{-5}/\varepsilon$ °K (bandwidth of 1 Hz) or of

$10^{-6}/\epsilon$ °K for lock-in detection system with time constant of 10 sec. and 12 db/oct roll-off (bandwidth = 1/8 x time ct). We note that the result is strongly dependant upon the emissivity of the surface: for the plastic samples used in this project ϵ is $\sim$ 1, for polished aluminium and steel it is of the order of 0.05 - 0.1 and for oxidized steel $\sim$ 0.7. We note also that this detection system has a detectivity about 10 times worse th n the microphone system.

IV. 3. Other thermometric systems

A system which detects the periodic thermally induced strain created by ultrasonic absorption has been also considered. A schematic of such a system is shown in Fig. 6:

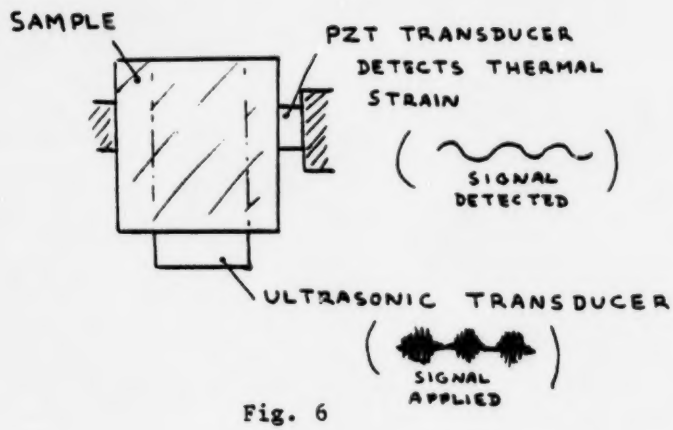

Fig. 6

The problem with this system arises from the parasitic strain produced by the heat generated in the coupling medium between the transducer and the sample. So far, no simple solution has been found to solve this problem in general. We should note however that a successful experiment has been reported recently by exciting at resonance a fused quartz sample [26]. Therefore, it is likely that such a system works if the sample is made with parallel surfaces and if a lower ultrasonic frequency is used (giving low absorption and especially low scattering and consequently high Q). In another system, used in the medical field [27], one measures the local temperature inside the sample with an additional low intensity

ultrasonic beam (see Fig. 7). The change of temperature produces a slight change of ultrasonic velocity which can be detected in principle, by a phase sensitive technique. The measurement is also affected by the strains induced by the heat generated by the beam and the coupling medium. So far, no solution has been found to eliminate the effect of the coupling medium.

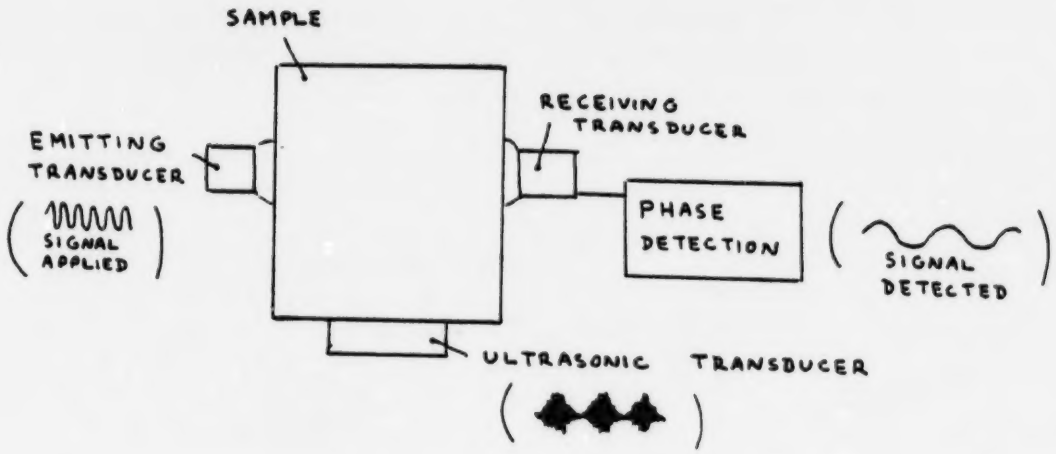

Fig. 7

V. EXPERIMENTAL RESULTS

In this section, we present several experimental results obtained with plastic samples (plexiglas, unplasticized polyvinylchloride), which have strong ultrasonic absorption and with a sample of cold rolled mild steel (1030/40) excited at mechanical resonance. A microphone thermometric system and a pyroelectric infrared detector have been used. We present also an example of application of the technique, namely the measurement of the ultrasonic absorption of a metallic glass ribbon as a function of the applied magnetic field.

V. 1. Microphone thermometric system

V. 1. a. Experiments with compressional waves

Early experiments made use of commercial transducers of KB-Aerotech. The experimental set-up used at this time is sketched in Fig. 8. The experimental results (signal magnitude versus modulation frequency) are plotted in Fig. 9 for the cell filled with ambiant air at atmospheric pressure. The sample is made of plexiglas. Its thickness (5.72 mm) is $\sim 50\ \mu_s$ at the lowest frequency used (2 Hz), so the thermal wave generated by the coupling fluid and the plastic cap of the transducer cannot be detected. We have verified that the signal vanishes when the cell is evacuated and is opened (in this case, it is very noisy since the microphone picks up ambiant noise). We have also verified that there is a quadratic dependance of the signal with the amplitude of the RF voltage applied to the transducer. These observations prove that the observed signal is really produced by pressure waves in the gas and has a thermal origin.

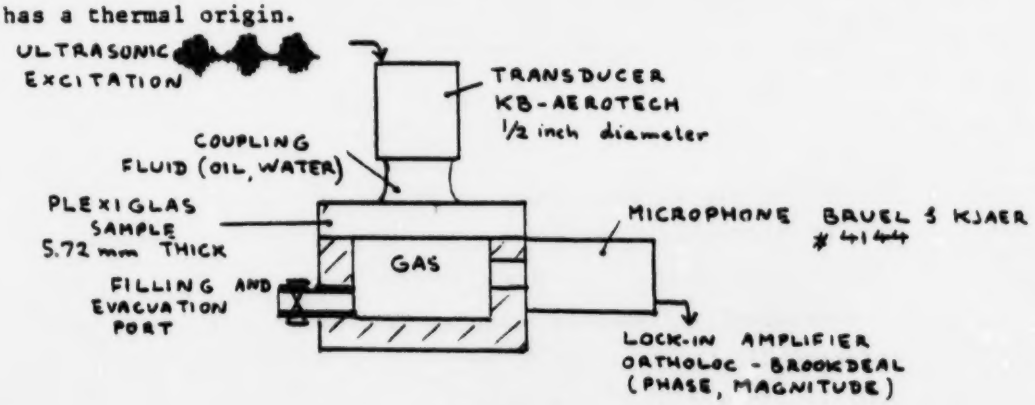
ULTRASONIC EXCITATION
TRANSDUCER KB-AEROTECH 1/2 inch diameter
COUPLING FLUID (OIL, WATER)
PLEXIGLAS SAMPLE 5.72 mm THICK
MICROPHONE BRUEL & KJAER # 4144
GAS
FILLING AND EVACUATION PORT
LOCK-IN AMPLIFIER ORTHOLOC - BROOKDEAL (PHASE, MAGNITUDE)

Fig. 8 Experimental set-up

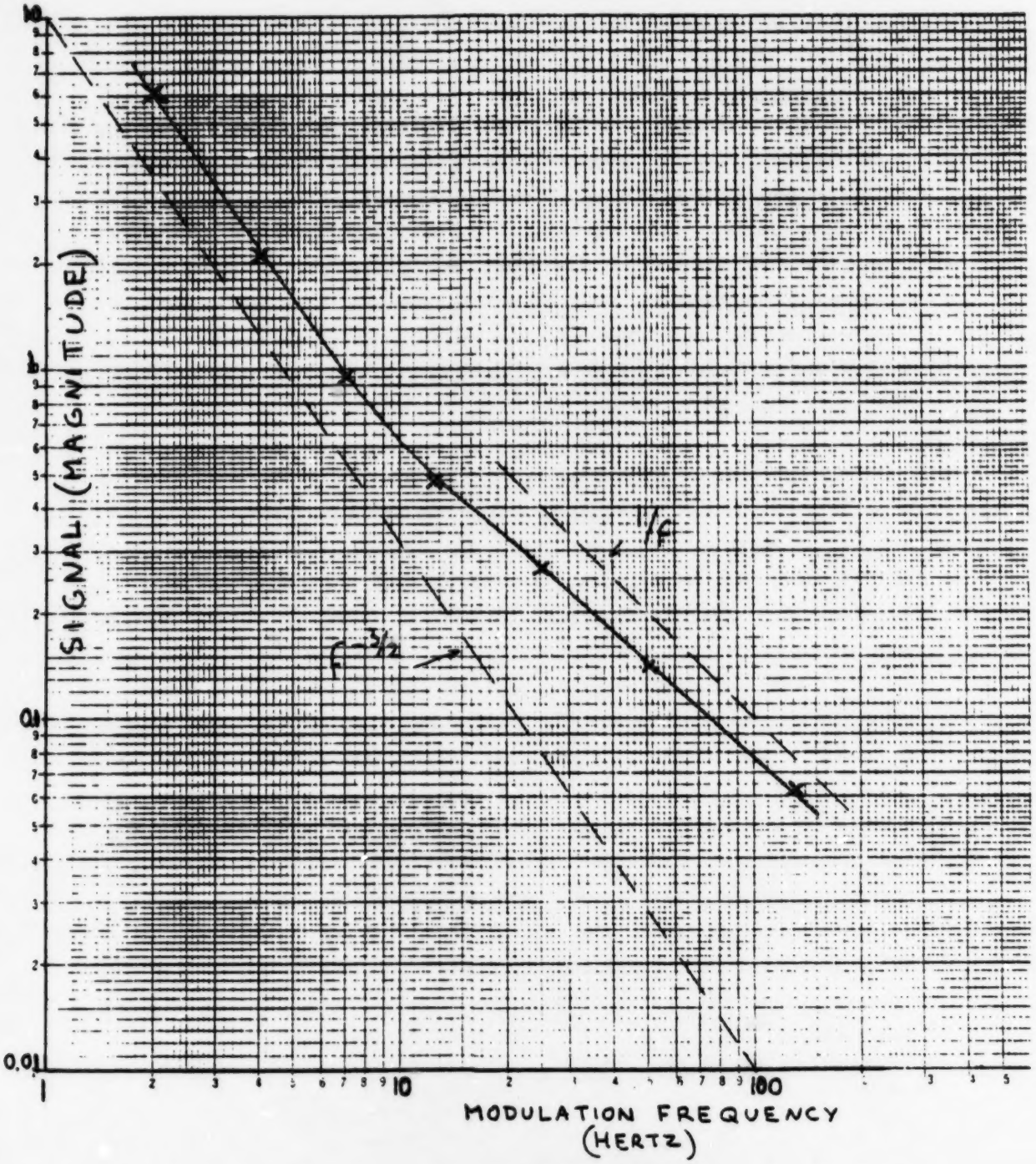

Fig. 9 Microphone signal as a function of the modulation frequency: air at atmospheric pressure (humidity unknown), transducer KB-Aerotech Alpha 5 MHz excited at f_u = 4 MHz (compression), plexiglas sample, ordinate unit = 1 volt corresponds to 2×10^{-3} Pa $\sim 2 \times 10^{-8}$ atm, noise $\sim$ 0.02 V_{rms} $\sim 4 \times 10^{-10}$ atm rms.

The results of Fig. 9 seem to agree with the theoretical predictions of section IV, namely a variation as $f^{-3/2}$ at low frequency where sample absorption is preponderant and as f^{-1} at higher frequency where gas absorption becomes larger. Data obtained with helium as filling gas seem also to confirm the predictions of section IV. However when commercial transducers operating at 2.25 MHz and 10 MHz were used very different frequency variations were observed: $\sim f^{-2}$ at 2.25 MHz and $\sim f^{-1}$ at 10 MHz below 20 Hz with the same plexiglas sample. With a sample of UPVC of approximately the same thickness, $\sim f^{-2.3}$ was observed at 2.25 MHz and at a low modulation frequency. A similar variation was observed at 2.25 MHz with an inch thick plexiglas sample. These observations do not correspond at all to the theoretical predictions of section IV. The cause does not seems to be a bending motion of the sample, because the same variation was observed with a very thick plexiglas sample. It was then speculated that the periodic strain at frequency f in the sample, or in the coupling fluid, or in the transducer and which is caused by the heating of the coupling fluid or of the transducer or plastic elements inside the transducer, is transmitted to the gas and is a cause of the observed frequency variation. In order to try to elucidate this question, bare X-cut crystal quartz transducers were later used. The coupling medium was either Nonaq grease or a high vacuum grease. With these transducers, also, no final and complete interpretation could be obtained. We reproduce in Fig. 10, data obtained at 5 MHz with one inch thick plexiglas sample and in Fig. 11, data obtained at the same frequency with the 5.72 mm thick plexiglas sample. When dry air is replaced by helium, we noticed a decrease of the signal (see Fig. 10 and 11), which shows that absorption by the gas constitutes a significant part of the signal (if solid absorption was preponderant, we should have seen an increase by the ratio of the $\gamma \mu_g$, which is 1.63 x 7000/(1.4 x 2600) $\sim$ 3). This assumption is confirmed when the signal is measured as a function of air pressure P_o inside the cell. At 2 Hz, we observe a rapid variation, approximately as P_o^2 (see Fig. 12). Since $Z_g/\rho_o C_p$ is independant of pressure, since μ_g varies as $P_o^{-1/2}$ and α_g as $1/P_o$ [28], Eq 64 indicates that the

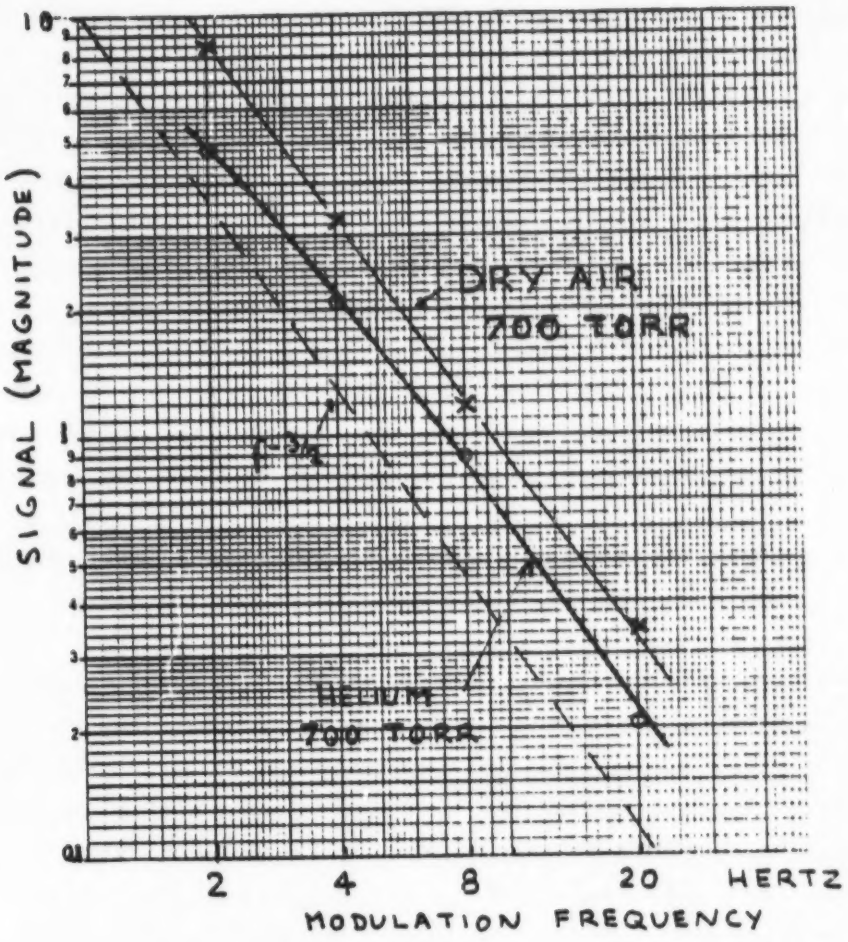

Fig. 10 Microphone signal as a function of the modulation frequency, sample: plexiglas 1 inch thick, transducer: quartz X-cut, 5 MHz, beam spot diam. = 1/2 inch, bonded with Nonaq grease, other side free.

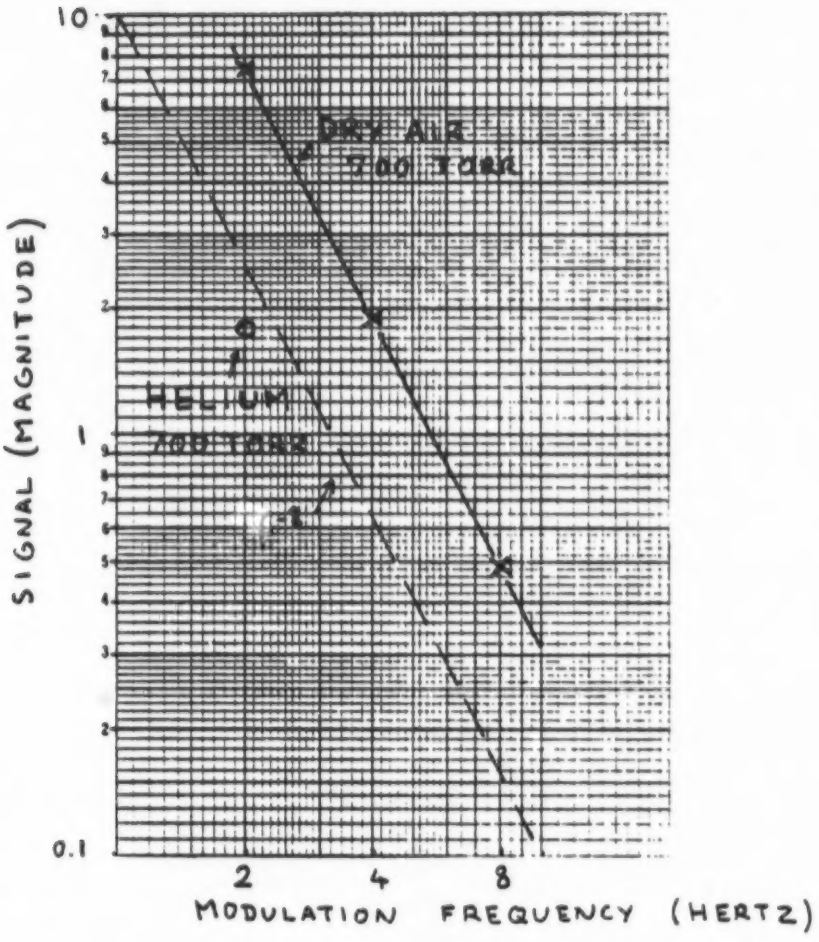

Fig. 11 Microphone signal as a function of the modulation frequency, sample: plexiglas 5.72 mm thick, transducer: quartz X-cut, 5 MHz, beam spot diam. = 1/4 inch, bonded with high vacuum grease, other side free.

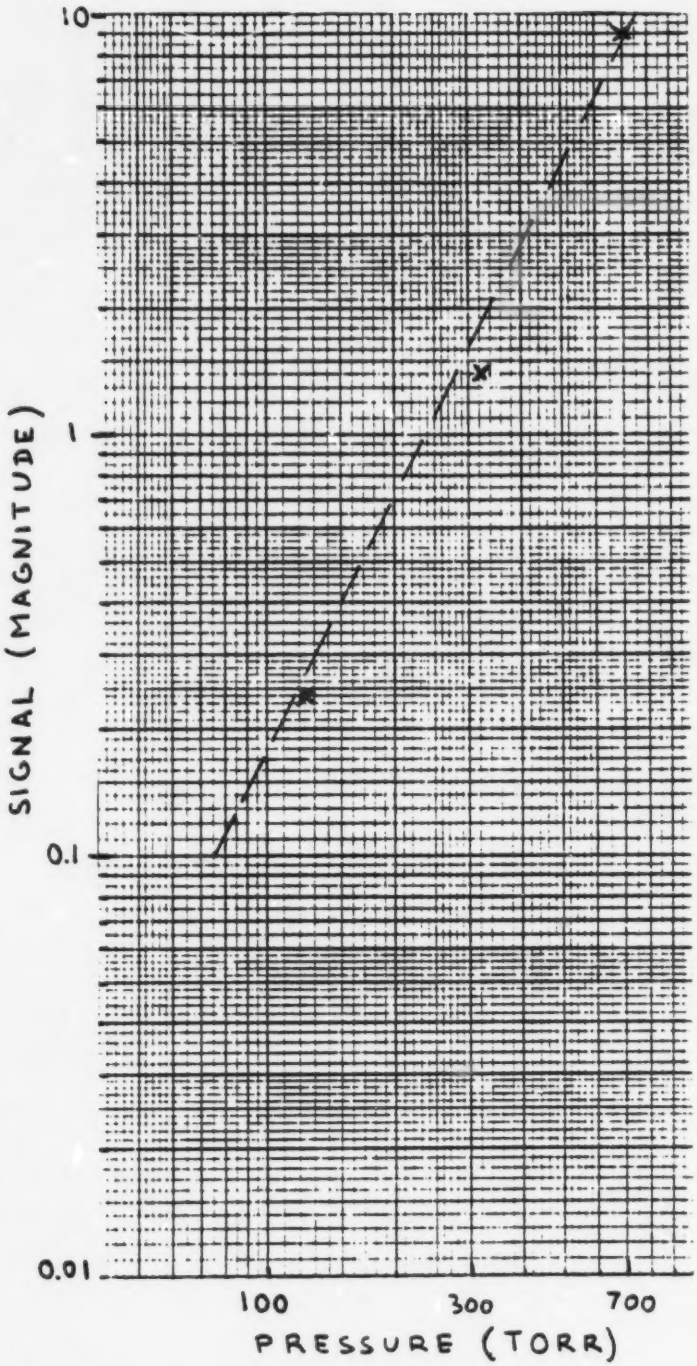

Fig. 12 Microphone signal at 2Hz modulation frequency, plotted as function of cell pressure (dry air); same sample and same transducer as for Fig. 11.

solid absorption term gives a variation as $\sqrt{P_o}$ whereas the gas absorption term gives a rapid variation as $P_o^{5/2}$. Therefore for this matter, we can say at least that there is no strong disagreement between theory and experiment. Also, when a weakly absorbing sample (fused quartz wedge) is used, a variation with frequency as $\sim f^{-1}$ is observed (see Fig. 13), in qualitative agreement with the predictions of the theory (Eq 78).

In conclusion, a comprehensive interpretation of the experimental results was not obtained, but we can say that the system using a microphone is not appropriate for measuring the absorption of longitudinal ultrasonic waves in a solid. The fact that absorption in the gas contributes to a large part of the signal could to be used for another application, namely the construction of a phase insentive ultrasonic detector, which may be of some interest for some applications [28].

V. 1. b. Experiments with shear waves

With shear wave excitation, the theory of section IV predicts a frequency variation as $f^{-3/2}$. This is reasonably verified by the data we present below. In Fig. 14, we plot the signal versus modulation frequency obtained at 5 MHz with a plexiglas sample 5.72 mm thick and in Fig. 15, we plot the data obtained at the same frequency with one inch thick mild steel (1030/40) sample excited at resonance. In both cases, we have used an AC-cut quartz transducer bonded with a low melting point agent (Crystalbond 509). However, we observe in Fig. 14 some discrepancy between magnitudes recorded in helium and in air: their ratio is $\sim$ 2.1 instead of 3, which may indicate that another heat source is produced.

V. 2. Infrared emissivity thermometer

The schematic of the experimental set-up is shown in Fig. 16.

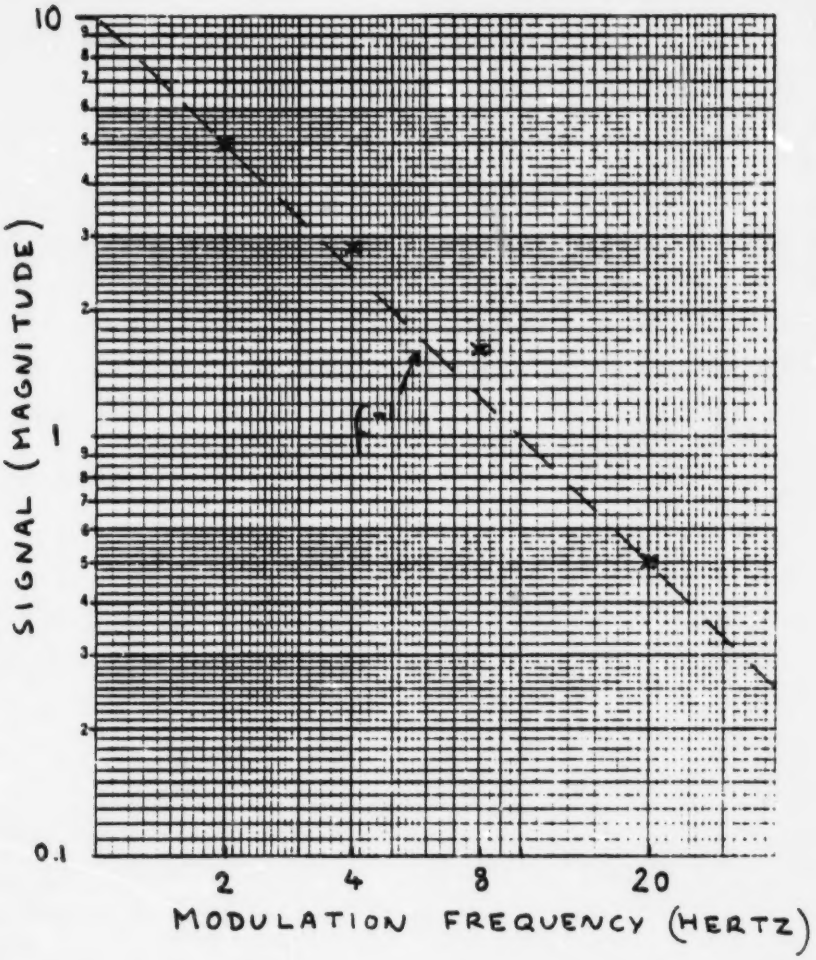

Fig. 13 Microphone signal as a function of the modulation frequency, sample: fused quartz ∿ 6 mm thick with ∿ 0.5° wedge, transducer: quartz X-cut, 5 MHz, beam spot diam. = 1/4 inch, other side free, bonded with high vacuum grease.

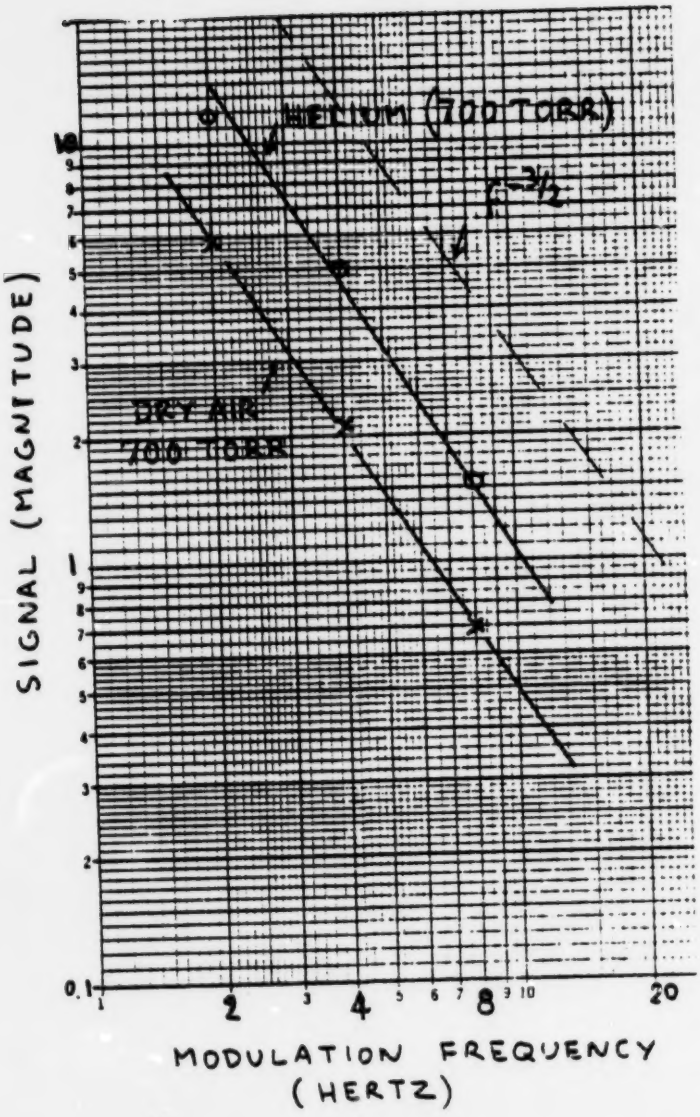

Fig. 14 Microphone signal versus modulation frequency, sample: plexiglas 5.72 mm thick, transducer: quartz AC-cut, 5 MHz, beam spot diam. = 1/4 inch, other side free, bonded with Crystalbond 509.

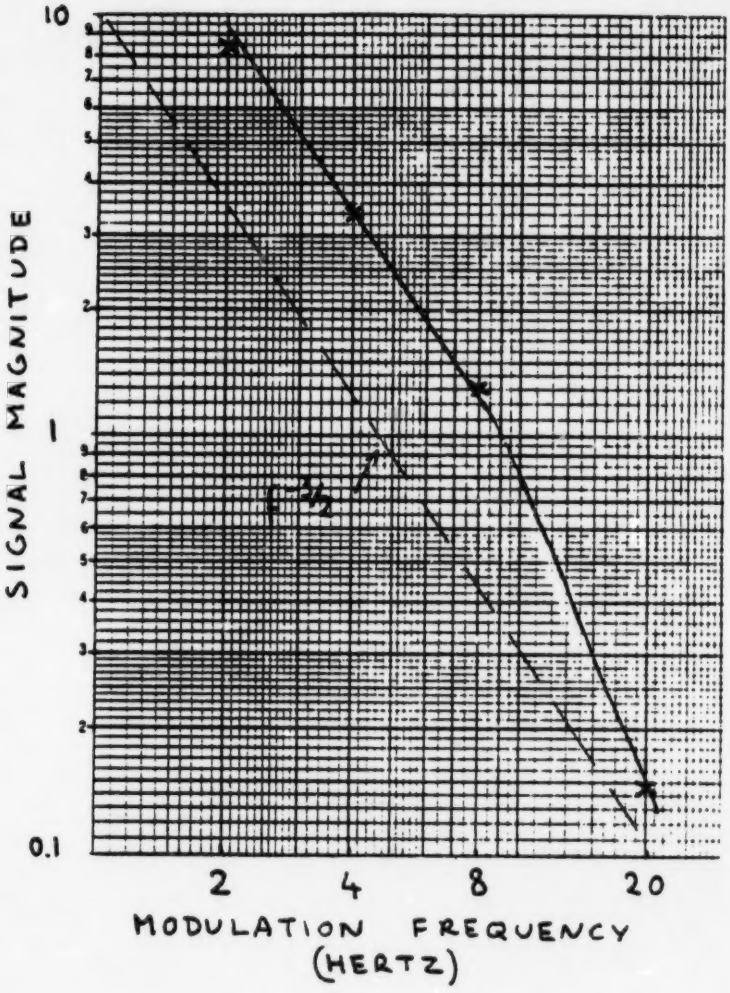

Fig. 15 Microphone signal versus modulation frequency, sample: mild steel 1030/40 one inch thick, transducer: quartz AC-cut, 5 MHz, beam spot diam. = 1/2 inch, other side free, bonded with Crystalbond 509.

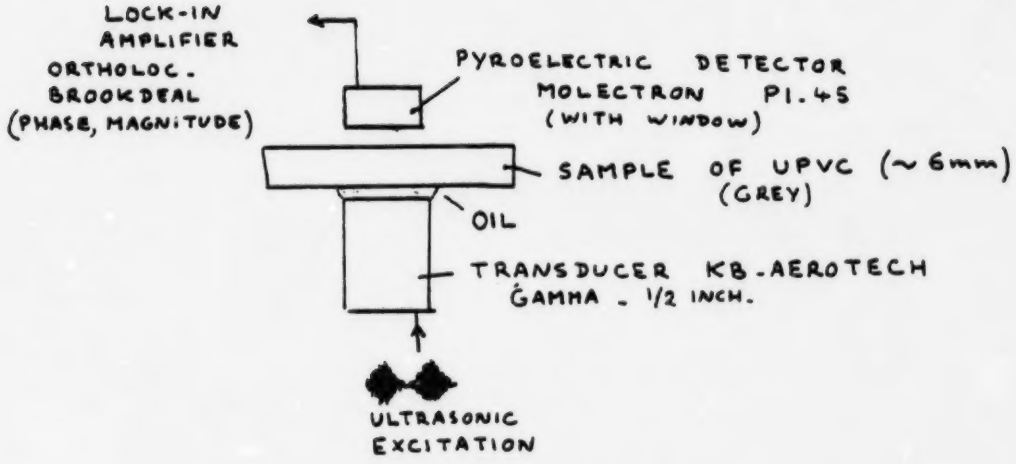

Fig. 16 Experimental set-up

The experimental results (signal magnitude versus modulation frequency) are plotted in Fig. 17. The sample thickness is such that the thermal wave produced by the coupling fluid and the transducer cannot be detected. We have verified that the signal vanishes when the detector field of view is masked. If detector response varies as $1/f$, we should expect a variation as $1/f^2$ according to Eq 81. Actually, the detector response falls off at low frequencies so we had to calibrate it. Its response curve is shown in Fig. 18. When this calibration data is used to correct the magnitude, we observed to a reasonable accuracy the expected $1/f^2$ frequency variation. Other data were taken with a smaller size detector (detector P1-43, diameter = 3 mm) and gave the same satisfactory results, i.e. a $1/f^2$ variation between 0.5 Hz and 50 Hz.

We have also tried a gold-doped germanium detector at 77°K. In this case, the detectivity is much lower than with pyroelectric detector. This was expected because of the large 1/f noise and also because the detection bandwidth of this detector is not optimum for room temperature detection (approximately between 1 to 10.6 μm).

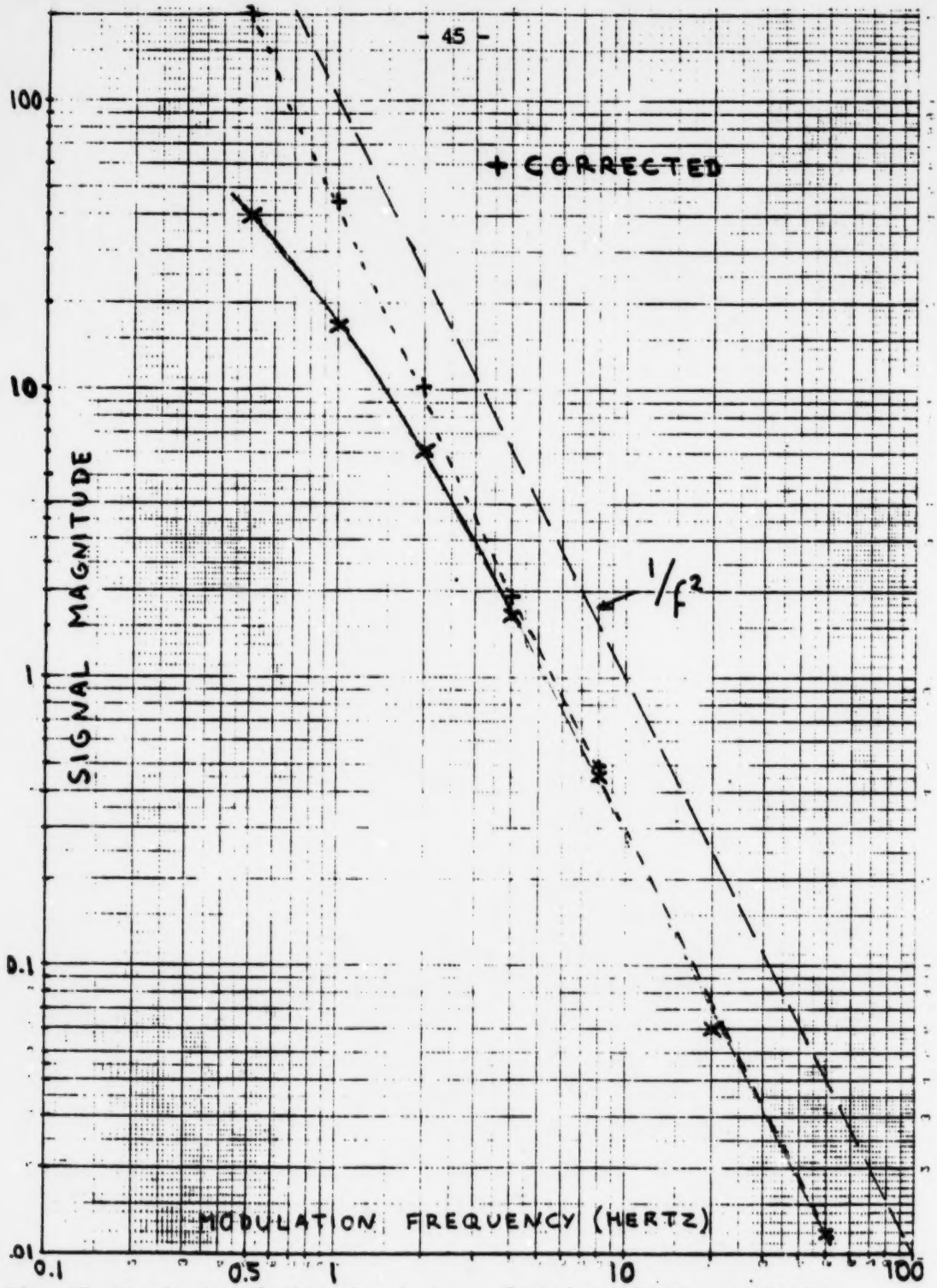

Fig. 17 Magnitude of the signal as a function of the modulation frequency: pyroelectric detector Molectron P1-45 diam. 5 mm, transducer KB-Aerotech, Gamma 2.25 MHz excited at 2.27 MHz, the signal at 1 Hz is ∿ 13.4 mV and corresponds to ∿ 1.2 x 10^{-7}W. The corrected points (+) take into account the deviation of the detector response from 1/f (see Fig. 18).

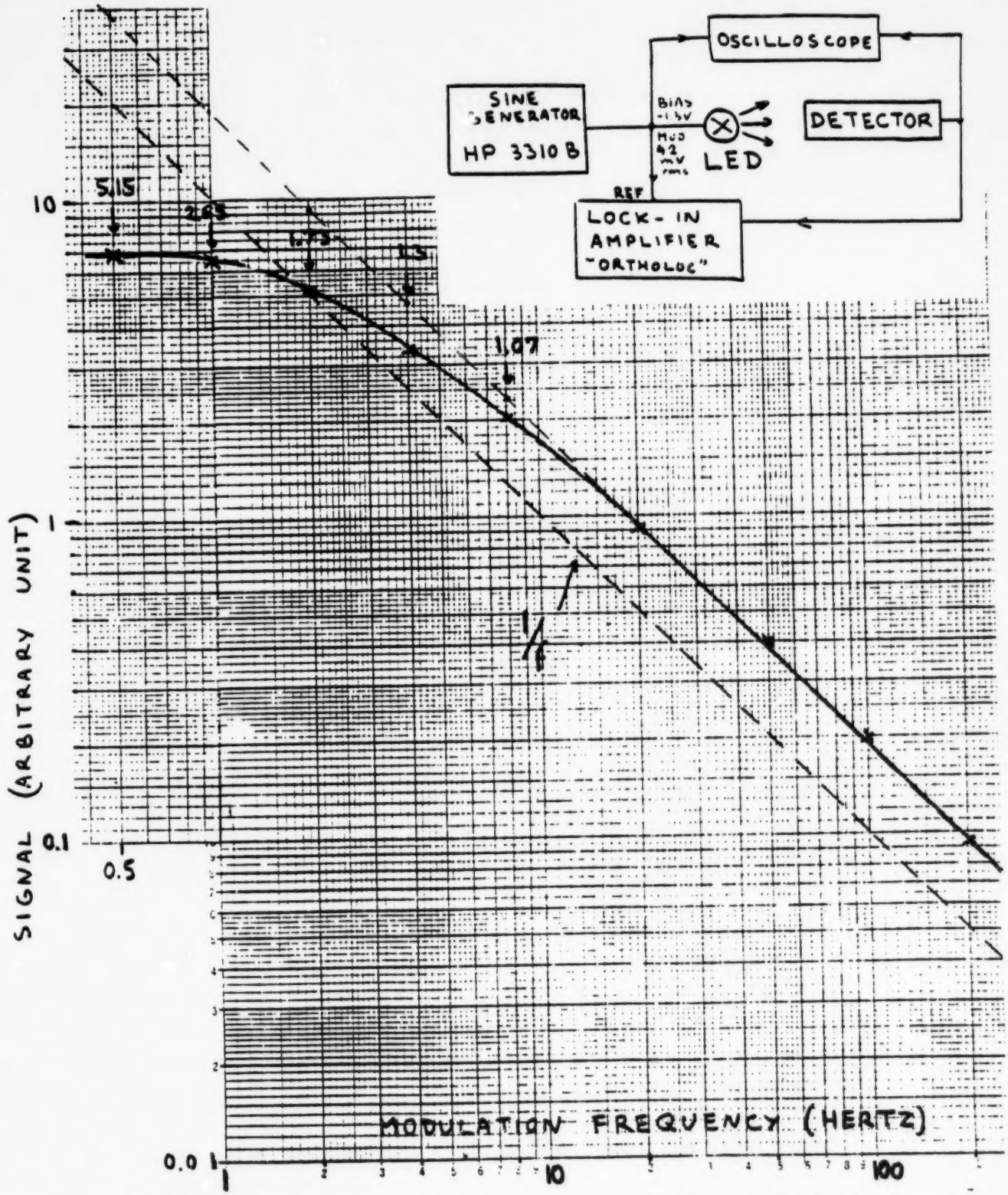

Fig. 18 Calibration curve of the response of the pyroelectric detector Molectron P1-45 diam. 5 mm. The insert shows the experimental set-up. The correction factors to a 1/f response are also indicated.

We have also performed a few experiments with a fused quartz sample (buffer rod, 1/2 inch thick). It was first observed that a strong signal was detected when the detector looks directly at the transducer, the signal being generated by the plastic cap of the transducer. When the fused quartz sample is coupled to the transducer on the top of it, the signal vanishes as expected, since fused quartz cuts off the infrared emission from the transducer above 4 μm and since its ultrasonic absorption is very low. If a drop of water, a layer of oil or grease, a paint layer or a piece of black electric tape are then applied on the surface of the quartz sample a strong signal is observed again. This signal is caused by the absorption by the surface layer. This shows that in practice interference free signals would be obtained only with clean surfaces. By tuning the ultrasonic frequency, large signal peaks are observed. We have verified that they are spaced by the fundamental resonance frequency of the quartz buffer. This shows that much larger signals would be observed if the sample can be set into resonance, but this will generally required end faces with a high degree of parallellism.

We have also observed with a pyroelectric detector (detector PI-43) the ultrasonic absorption of a mild steel sample (1030/40, one inch thick) using compression and shear waves. The sample has been machined with two parallel surfaces. The surface viewed by the detector has been darkened to increase its emissivity by dipping the sample into nital. Fig. 19 shows the results obtained by exciting the sample with a commercial compression transducer at 2.25 MHz. Fig. 20 shows data obtained with a shear transducer at 5 MHz bonded to sample. In both cases, their is a reasonable agreement with theory concerning the signal magnitude variation. The observed phase is also in agreement with that observed with the plastic (UPVC) sample.

These experiments performed using a pyroelectric detector and plastic and steel samples confirm that the emissivity thermometric system measures truly the ultrasonic absorption of the solid and that its sensivity is sufficient to perform experiments on steel samples.

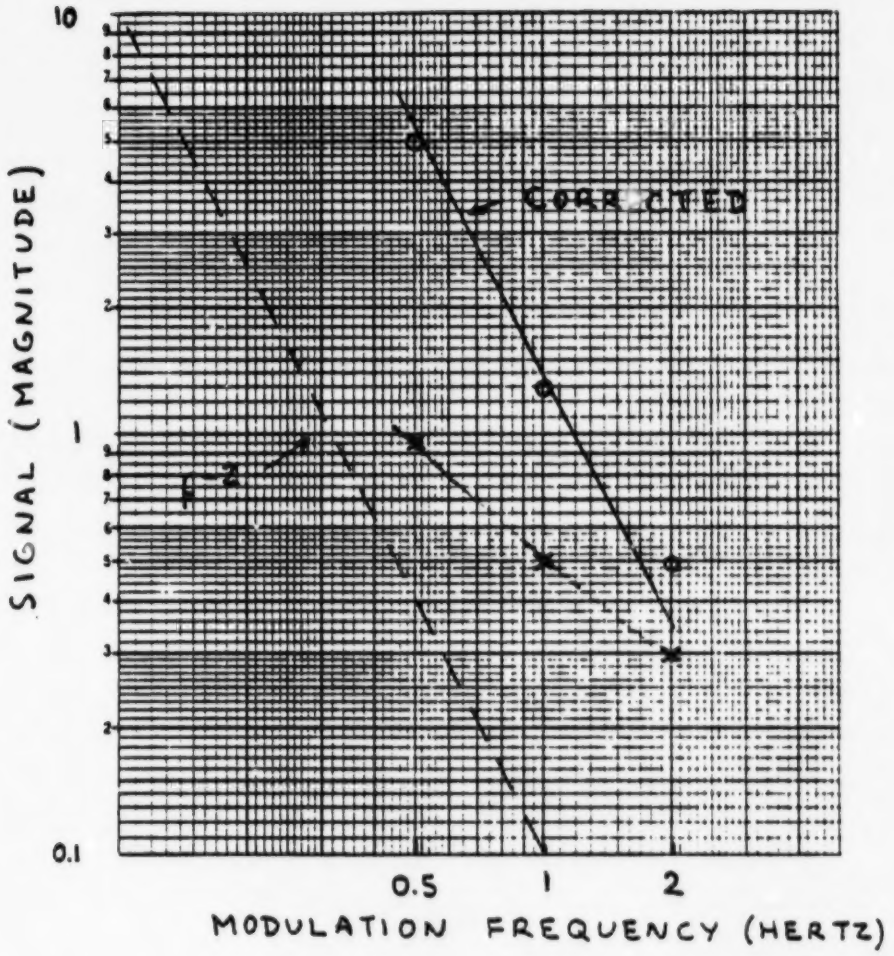

Fig. 19 Pyroelectric (P1-43) signal versus modulation frequency, sample: mild steel (1030/40) 1 inch thick excited at resonance, transducer: KB-Aerotech Gamma 2.25 MHz, oil coupling, uses a 3 watts 37 dB RF amplifier.

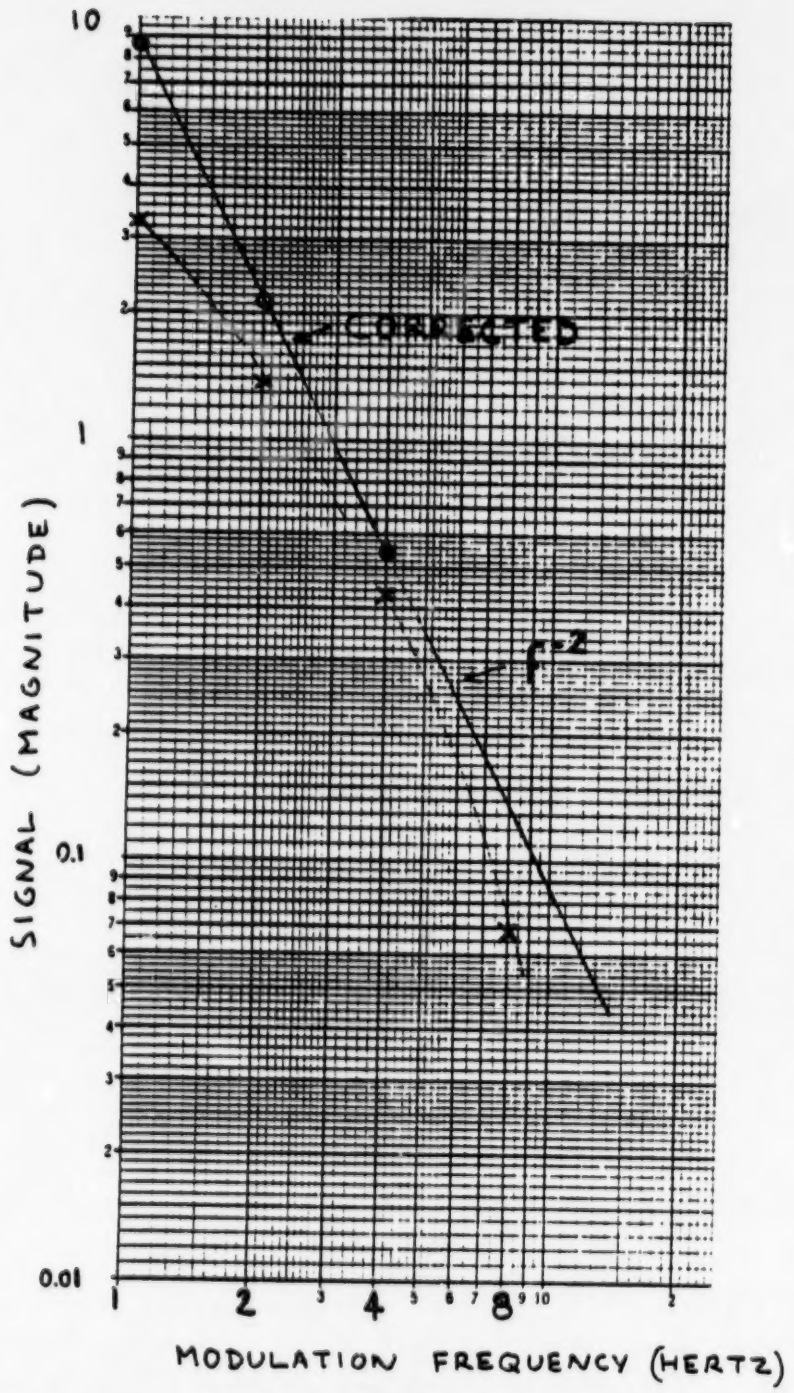

Fig. 20 Pyroelectric (P1-43) signal versus modulation frequency, sample: mild steel (1030/40) 1 inch thick excited at resonance, transducer: quartz AC-cut 5 MHz, beam spot diam. = 0.5 inch, bonded with Crystalboard 509, uses a 150 watts 57 dB RF amplifier.

V. 3. An example of application of the technique: detection of the ultrasonic absorption of a metallic glass ribbon in a magnetic field.

This experiment uses as sample an as-quenched amorphous Metglas ribbon (2605SC of Allied Chemical Co.) which is placed between the poles of an electromagnet. A 5 MHz shear wave transducer (Lithium Niobate) is glued at one end of a 7 cm long piece and is used to launch SH waves along the ribbon. A pyroelectric detector PI-45 detects the emitted radiation from a region in the middle of the ribbon. The RF power is modulated at ∿ 2Hz and we have used phase sensitive detection at this frequency. Ultrasonic absorption is caused in part by magnetic domaines motion [30]. At zero field, it is very large [31], so there is no propagation along the ribbon. At high field, it should reach a constant value, since there are other causes of absorption.

The experimental results are plotted in Fig. 21. As expected no signal is seen at zero field, there is a rapid increase of a signal with increasing field (see ref. 31) and there is a constant asymptotic value at high field. We observe also a maximum which can be explained by the theory of section III. Since the ribbon is not cut precisely perpendicular to its edge and, since also the transducer is not precisely perpendicular to it, no resonance effect takes place in the ribbon, so Eq 46 and 47 apply. Therefore the heat source varies as $\alpha \cosh 2\alpha z/\cosh 2\alpha \ell$ or $f(z/\ell, a) = a \cosh az/\ell \,/\, \cosh a$ where $a = 2\alpha\ell$ (z is measured form the end at the opposite side from the transducer). It can be readily shown that the function $f(z/\ell, a)$ has an extremum at the value $a = a_M$ such that $a_M = 1 \,/\, [\tanh a_M - z/\ell \tanh (z/\ell\, a_M)]$. For $z = 0$, $a_M \sim 1.2$ and $f(0, a)$ is plotted in Fig. 22. If α is a monotoneously decreasing function of the applied magnetic field H [31], it then results a maximum when the signal is plotted as a function of H, as it can be seen in Fig. 21.

Actually, we detect all the radiation emitted by a finite area defined by coordinates z_1 and z_2. In this case, it can be readily shown that the signal is proportional to the function $F(z_1/\ell,$

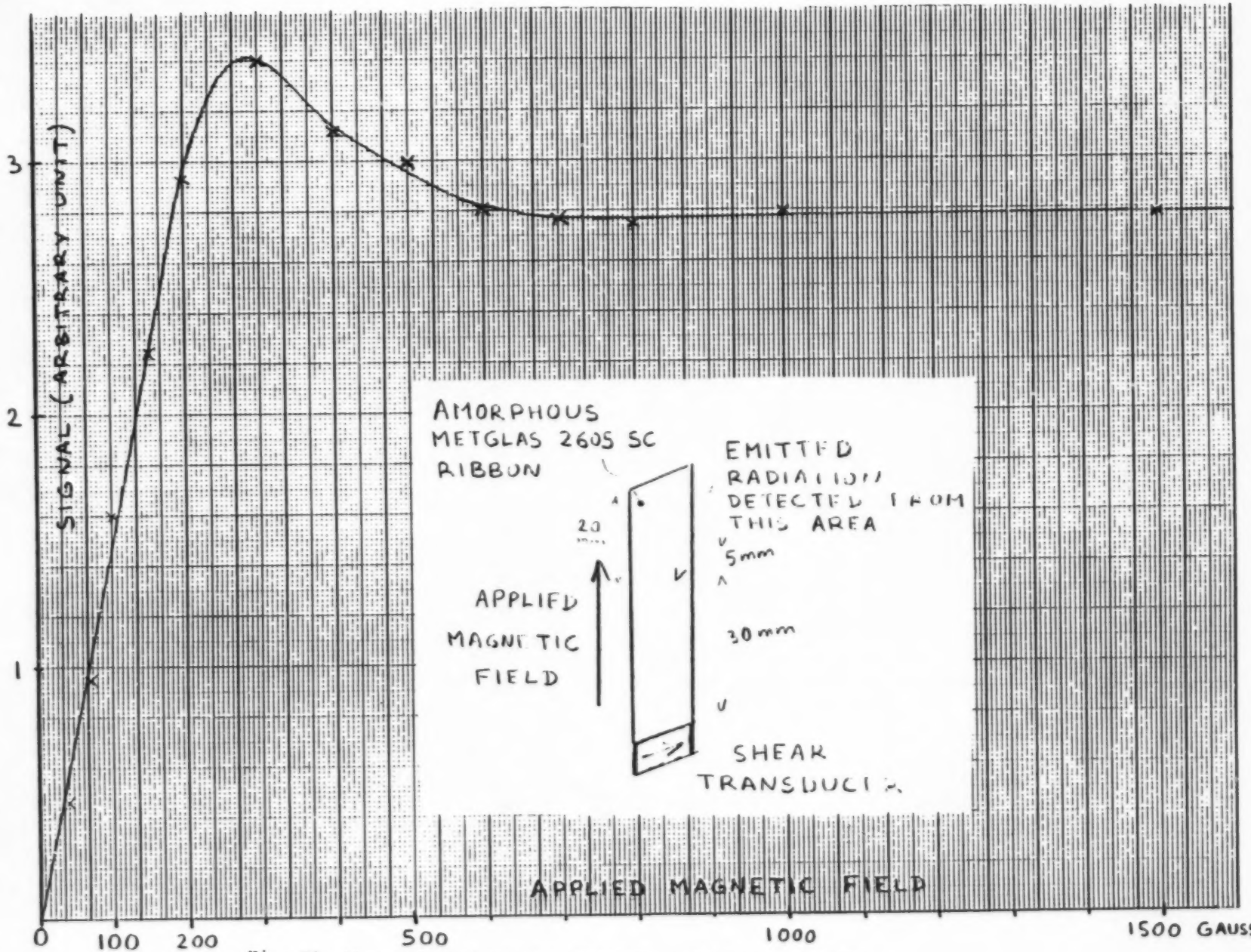

Fig. 21 Absorption of Metglas 2605 SC, SH waves at 5 MHz.

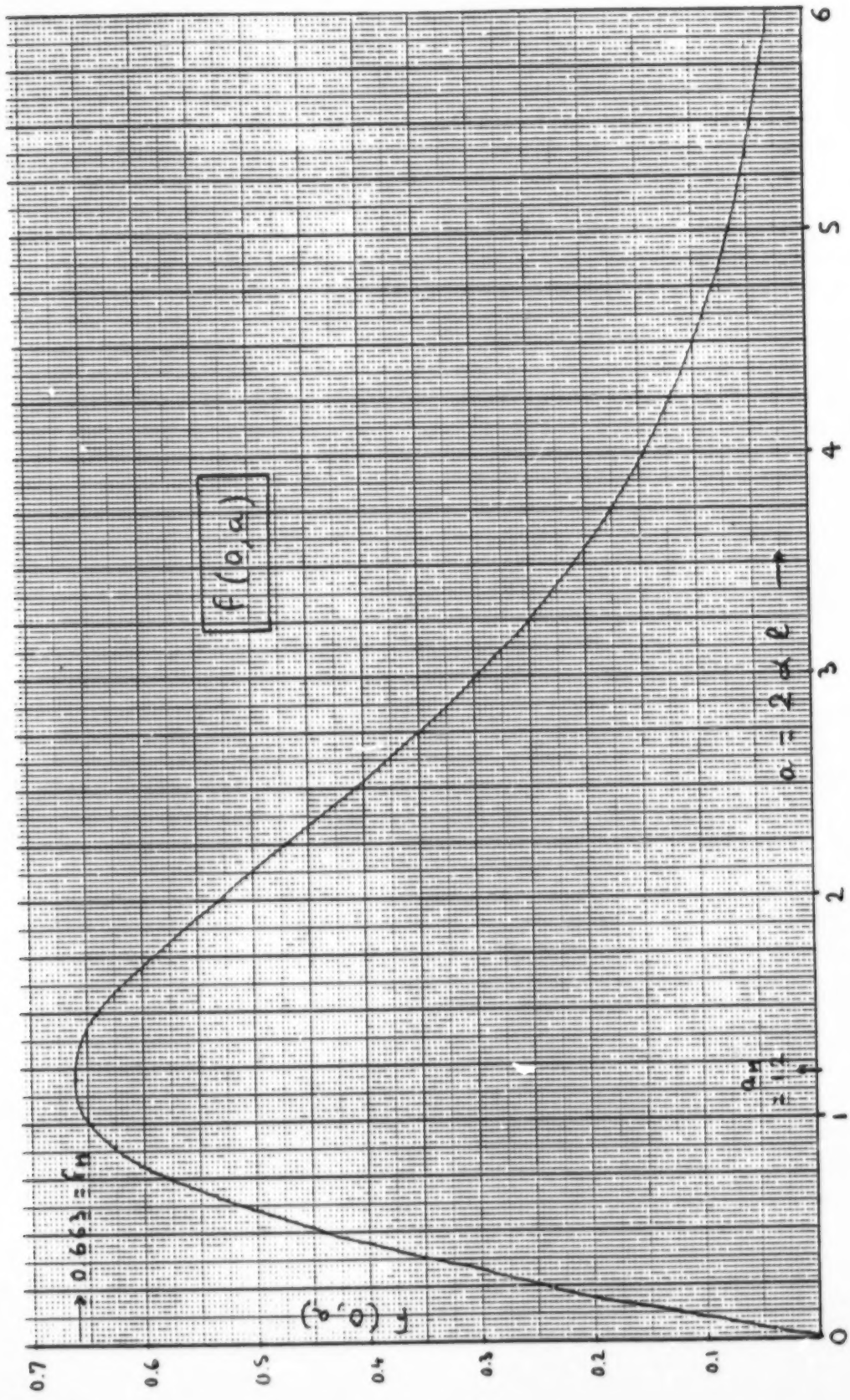

Fig. 22 Plot of f(0, a) versus a.

z_2/ℓ, a) = [sinh az_2/ℓ - sinh az_1/ℓ]/cosha . For z_2-z_1 small, $F(z_1/\ell,\ z_2/\ell,\ a) \sim [(z_2-z_1)/\ell]$ f $(z_1-z_2/2\ell,\ a)$. The data of Fig. 20 have been taken with ℓ = 55 mm, z_2 = - 20 mm, and z_1 = - 25 mm, so z_1/ℓ = - 0.4545, z_2/ℓ = - 0.3636, $(z_2-z_1)/\ell$ = 0.0909 and $(z_2+z_1)/2\ell$ = - 0.4091 (it would have been simpler to measure the radiation emitted from the end of the ribbon: z_2 = 0). The function F $(z_1/\ell,\ z_2/\ell,\ a)$ is plotted in Fig. 23 for the actual experimental values of ℓ, z_1 and z_2. The experimental data are then normalized to the maximum value F_M of F. Using the curve plotted in Fig. 23, we then deduce for each experimental point the corresponding value of a; this gives α, ℓ being known. The results, α versus the magnetic field, are plotted in Fig. 24.

There is a qualitative agreement between these results and those recently published by M. Poirier et al [31]. However, he reported a dip between 100 and 200 gauss which may has been missed because an unsufficient number of data points have been recorded. We have also operated at 5 MHz instead of 3.6 MHz, so the dip should be more shallow [31]. We note that we are able to obtain the absolute value of the absorption coefficient. This is not possible by a simple transmission measurement (one transducer emitter at one end of the ribbon and one transducer-receiver at the other end). By pulse-echo, two echos are at least required. Even in this case the measurement is complicated by orientation problems of the transducer and of the end cut. These problems arise because the detection is performed with a piezoelectric crystal which is a phase-sensitive device. In our case, the detection is instead truly phase-insensitive.

In conclusion, we have devised a new technique for measuring the absorption of ultrasonic waves launched along a Metglas ribbon, this technique is based on the detection of thermo-emission from the ribbon.

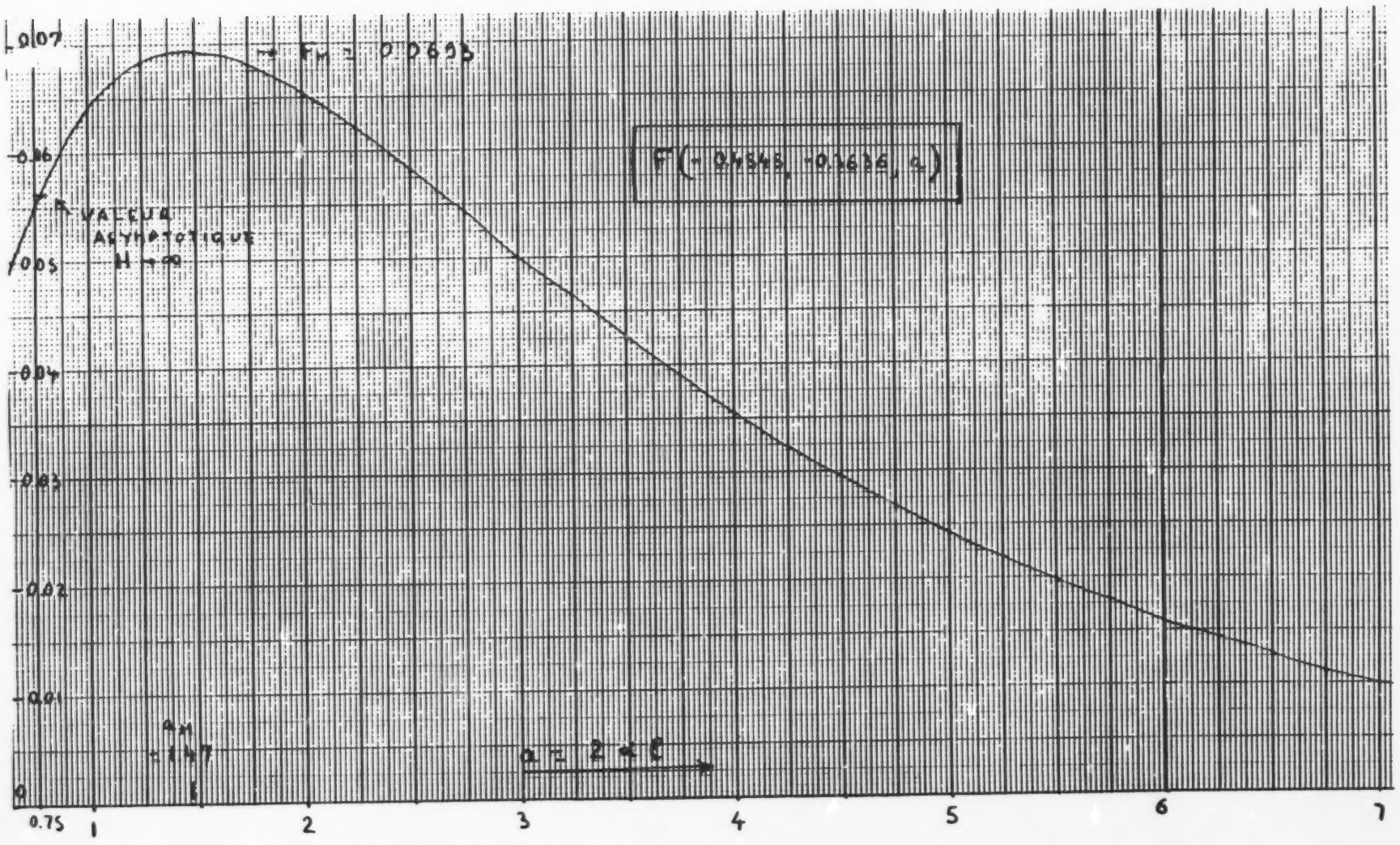

Fig. 23 Plot of $F(z_1/\ell, z_2/\ell, a)$ versus a for z_1/ℓ = - 25/55 and z_2/ℓ_2 = - 20/55.

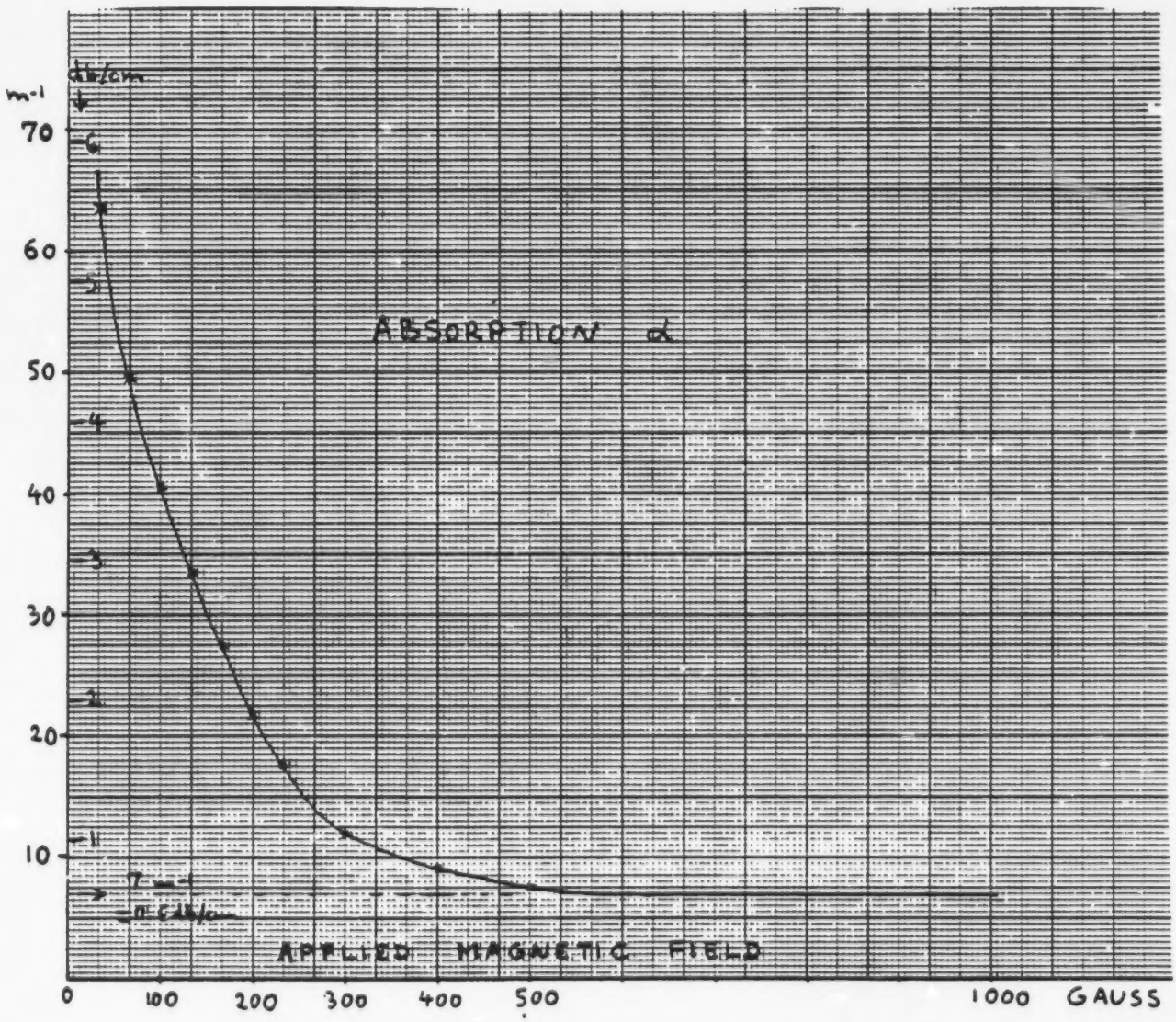

Fig. 24 Absorption coefficient α (for the stress) versus applied magnetic field, SH mode, 5 MHz, ribbon of Metglas 2605 SC, field parallel to the ribbon.

VI. CONCLUSION AND PERSPECTIVES

Three main conclusions and directions for future development follow from this work:

1. The microphone thermometric system, which is a very sensitive device, has been shown to be in general inappropriate for the measurement of ultrasonic absorption (except for shear waves at normal incidence). We have noticed that the signal is caused in large part by absorption by the gas of the cell. This fact and the sensitivity of the device suggests the possibility of its application to phase insensitive detection of ultrasonic attenuation (by measuring the ultrasonic power arriving at a surface). However, since a satisfactory interpretation of experimental data was not obtained, further studies should be conducted for this purpose (in particular, in order to determine the modulation frequency to be used). Such a device which would work with continuous ultrasonic excitation is potentially useful for resonance experiments and for transmission measurements in large plates, where parasitic reflections do not interfere (e.g. rolled slabs or sheets). We remind that it has been shown that information on grain size and on several mechanical properties of steel can be obtained by measuring transmission or attenuation [1].

2. The thermo-emissive system has been shown to be appropriate for measuring ultrasonic absorption to a depth of a few mm in steel samples. As it was mentionned in the introduction, the ultimate objective is to apply this technique to the measurement of residual stresses and to the measurement of fatigue. Therefore, the next step will be to devise an experiment where one would observe the change of absorption caused by an externally applied stress. For this purpose, we plan to conduct a tensile test experiment (within the elastic limit) using a steel sample of square cross-section ($\sim$ 1/2 inch square): a transducer (compression or shear, quartz, lithium niobate or PZT-5) will be mounted on one side and the emissivity will be measured from the opposite side with an infrared detector (pyroelectric P1-45 or P1-75 of Molectron or Golay detector). The conditions to be satisfied in order to produce strong ultrasonic generation (in particular the choice of the transducer material) will be studied.

3. We have successfully applied the thermo-emissive technique to the measurement of ultrasonic absorption as a function of applied magnetic field in a Metglas ribbon. This technique gives an absolute value of the absorption coefficient and can work with a rather short sample (< 1 inch). The application of such a technique to steel samples shaped as plates seems to deserve some consideration and would be investigated to some extent.

	ρ	C	K	$\mu \times \sqrt{f}$	$R \times \sqrt{f}/(1-j)$	Z_{LONG}	Z_{SHEAR}	α_{LONG} (10MHz)		α_{SHEAR} (10MHz)	
	kg/m^3	J/kg.°K	W/m.°K	(μm)	$m^2.°K/W$	kg $m^{-2}s^{-1}$	kg $m^{-2}s^{-1}$	m^{-1}	db/cm	m^{-1}	db/cm
AIR 20°C, 1 atm	1.2	1003	2.59×10^{-2}	2617	5×10^{-2}	415	26.3	1.85×10^3	160	1.5×10^6	
HELIUM 20°C, 1 atm	0.18	5225	0.144	6970	2.42×10^{-2}	175	10.2	525	45.6	5.5×10^5	
ALUMINUM	2700	900	222	5390	1.215×10^{-5}	1.72×10^7	8.4×10^6				
CARBON STEEL(%) 0.8C, 0.1Cr 0.3Mn, 0.1Ni 0.1Si	7800	480	50	2060	2.06×10^{-5}	4.7×10^7	2.52×10^7			3 to 40	0.26 to 3.47
FUSED QUARTZ	2200	920	1.18	430	1.82×10^{-4}	1.31×10^7	8.28×10^6				
PLEXIGLAS (LUCITE) ACRYLIC	1190	1460	0.188	186	4.94×10^{-4}	3.15×10^6	1.29×10^6	104	9		
UNPLAST. POLYVINYL-CHLORIDE "JAYCOR"	1470	1004	0.167	190	5.7×10^{-4}	3.5×10^6		75 (2.25)	6.5 (2.25)		
WATER						1.48×10^6		2.5	0.217		

TABLE 1

ρ = density, C = specific heat, K = thermal conductivity, μ = thermal diffusion length, R = thermal impedance, Z_{LONG} = longitudinal acoustic impedance, Z_{SHEAR} = shear acoustic impedance (or η/μ_v), α_{LONG} = absorption coefficient for the stress (10MHz, longitudinal), α_{SHEAR} = absorption coefficient for the stress (10 MHz, shear or $1/\mu_v$); 1 m^{-1} (or 1 Neper/m) = 0.08686 db/cm.

Dry air (20°C, ref.[32]), $\alpha_{LONG} = 1.85 \times 10^{-11} \times f_u^2(m^{-1})$

Helium (20°C, ref[33]), $\alpha_{LONG} = 0.525 \times 10^{-11} \times f_u^2(m^{-1})$

Carbon steel (ref[34]), α_{SHEAR} between $3 \times 10^{-7} \times f_u(m^{-1})$ and $4 \times 10^{-6} \times f_u(m^{-1})$

Plexiglas (measured by pulse-echo): at 5 MHz, $\alpha_{LONG} \sim 58\ m^{-1}$, at 2.25 MHz, $\alpha_{LONG} \sim 27\ m^{-1}$

UPVC (measured by pulse-echo): $v_{LONG} \sim 2380$ m/s, $\alpha_{LONG} \sim 75\ m^{-1}$ at 2.25 MHz

Water (distilled, 20°C, ref[32]): $\alpha_{LONG} = 25 \times 10^{-15} \times f_u^2(m^{-1})$

REFERENCES

1. R. Klinman and E.T. Stephenson, Materials Evaluation, 39, 1116 (1981).
2. Ultrasonic Materials Characterization, Proceedings of the 1st International Symposium on Ultrasonic Materials Characterization, 1978, NBS Special Publication 596 (1980), see paper by A. Vary pp. 41-53.
3. K. Goebbels in Ref. 2, p. 37-40.
4. A.B. Bhatia, Ultrasonic Absorption, Clarendon Press, Oxford (1967).
5. E. Schneider, K. Goebbels, G. Hubschen and H.J. Salzburger, IEEE Ultrasonics Symposium Proceedings, 1981, p. 956.
6. K. Goebbels and P. Höller, in Ref. 2 p. 67-74.
7. R. Klinman, G.R. Webster, F.J. Marsh and E.T. Stephenson, in Ref. 2, p. 83-98.
8. S. Serabian, British J. of NDT. p. 69, vol. 22, (1980).
9. P.J.F. Forsyth, The Physical Basis of Metal Fatigue, Blade and Sons Ltd., London (1969).
10. G. Gremaud, Internal Friction and Ultrasonic Attenuation in Solids, Proceedings of the VIIth International Conference, J. de Physique (supplément), p. C5-1141.
11. E.G. Henneke II, K.L. Reifsnider and W.W. Stinchcomb, J. of Metals, sept 1979, p. 11.
12. H.S. Carslaw and J.C. Jaeger, Conduction of heat in solids, 2nd Edition, Oxford Press, 1959.
13. H.L. Libby, Introduction to Electromagnetic Non-destructive Test Methods, Wiley (New York), 1971.
14. E. Dieulesaint et D. Royer, Ondes élastiques dans les solides, Masson (Paris), 1974, chap. 5.
15. P. Cielo, Rapport intérimaire , Projet IGM 144, 30 juin 1981.
16. R. Dändliker and J.F. Willemin, Optics Lett. 6, 165, (1981).
17. E. Dieulesaint et D. Royer, Ondes élastiques dans les solides, Masson (Paris), 1974, chap. 7.
18. A. Rosencwaig, Photoacoustics and Photoacoustic Spectroscopy, vol. 57 in Chemical Analysis Series, J. Wiley, New York, 1980.

19. L.E. Kinsler and A.R. Frey, Fundamentals of Acoustics, J. Wiley, New York, 1962, 2nd Edition, chap. 5.
20. A.B. Bhatia, Ultrasonic Absorption, Oxford Press (1967), Chap. 4.4.
21. P.M. Morse and K.U. Ingard, Theoretical Acoustics, McGraw Hill, New York, 1968, Chap. 6.4.
22. J.-P. Monchalin, L. Bertrand and F. Lepoutre, to be published.
23. The infrared handbook, edited by W.L. Wolfe and G.J. Zissis, Environmental Research Institute of Michigan (1978), pp. 1-16, Fig. 1-8.
24. Molectron Corp., Specifications Sheet of Ultra-Low Noise Pyroelectric Detector/FET Preamp.
25. Cathodeon Corp., Specifications Sheet of the Low Noise IR50 Detector.
26. H.I. Ringermacher and J.S. Heyman, IEEE Ultrasonics Symposium Proceedings, 1981, p. 840.
27. T.D. Szchs, IEEE Ultrasonics Symposium Proceedings, 1973, p. 52.
28. R.T. Beyer and S.V. Letcher, Physical Ultrasonics, 1969, Academic Press (New York), Chap. 4.
29. J.S. Heyman and J.H. Cantrell, Jr., IEEE Ultrasonics Symposium Proceedings, 1979, p. 289.
30. R. Truell, C. Elbaum and B.B. Chick, Ultrasonics Methods in Solid State Physics, Academic Press, New York (1969), § 50
31. M. Poirier, J.D.N. Cheeke and L. Germain, Can. J. of Physics, 60, 385 (1982).
32. G.W.C. Kaye and T.H. Laby, Tables of Physical and Chemical Constants, 14th ed., Longmans, (1973).
33. Ref. 28, Chap. 4.
34. K. Goebbels and P. Höller, in Ref. 2, pp. 67-74.